MCB
Journals.ASM.org

KLF5 Activates MicroRNA 200 Transcription To Maintain Epithelial Characteristics and Prevent Induced Epithelial-Mesenchymal Transition in Epithelial Cells

Baotong Zhang,[a,b] Zhiqian Zhang,[a,b] Siyuan Xia,[a] Changsheng Xing,[a,b] Xinpei Ci,[a] Xin Li,[a] Ranran Zhao,[a] Sha Tian,[a] Gui Ma,[a] Zhengmao Zhu,[a] Liya Fu,[a] Jin-Tang Dong[a,b]

Department of Genetics and Cell Biology, College of Life Sciences, Nankai University, Tianjin, China[a]; Department of Hematology and Medical Oncology, Emory Winship Cancer Institute, Emory University School of Medicine, Atlanta, Georgia, USA[b]

KLF5 is an essential basic transcriptional factor that regulates a number of physiopathological processes. In this study, we tested whether and how KLF5 modulates the epithelial-mesenchymal transition (EMT). Using transforming growth factor β (TGF-β)- and epidermal growth factor (EGF)-treated epithelial cells as an established model of EMT, we found that KLF5 was downregulated during EMT and that knockdown of *KLF5* induced EMT even in the absence of TGF-β and EGF treatment, as indicated by phenotypic and molecular EMT properties. Array-based screening suggested and biochemical analyses confirmed that the microRNA 200 (miR-200) microRNAs, a group of well-established EMT repressors, were transcriptionally activated by KLF5 via its direct binding to the GC boxes in miR-200 gene promoters. Functionally, overexpression of miR-200 prevented the EMT induced by *KLF5* knockdown or by TGF-β and EGF treatment, and ectopic expression of KLF5 attenuated TGF-β- and EGF-induced EMT by rescuing the expression of miR-200. In mouse prostates, knockout of *Klf5* downregulated the miR-200 family and induced molecular changes indicative of EMT. These findings indicate that KLF5 maintains epithelial characteristics and prevents EMT by transcriptionally activating the miR-200 family in epithelial cells.

The basic transcriptional factor Krüppel-like factor 5 (KLF5, IKLF5, or BTEB2) is ubiquitously expressed in different tissues (1), including skin (2), lung (3), prostate (4), breast (5), and intestine (6, 7). It mediates or regulates diverse cellular processes, including proliferation, cell cycle, apoptosis, differentiation, and migration (8). Cellular migration, for example, appears to be regulated by KLF5 in a context-dependent manner (6, 9, 10), as KLF5 promotes cell migration in mouse primary esophageal keratinocytes by inducing the integrin-linked kinase (ILK) (10). Loss of *Klf5* could drive invasive progression of human squamous cell cancer in the context of *p53* ablation (11). The migratory ability of cells is often associated with epithelial-mesenchymal transition (EMT) during normal development and cancer progression (12), and KLF5 was predicted to be 1 of the 25 potential regulators of EMT predicted by a novel statistical method, NetworkProfiler, which predicts specific gene regulatory networks for a specific tumor characteristic on the basis of gene expression data (13). KLF5 belongs to the Krüppel-like factor (KLF) family (14), which has several members that regulate EMT, including KLF4 (15, 16), KLF8 (17, 18), and KLF17 (19). In particular, KLF5 and KLF4 have both similarities and distinctions in the regulation of cell proliferation (20) and stemness maintenance (21). These findings suggest a role of KLF5 in EMT regulation. Together with the findings that KLF5 regulates the proliferation and differentiation of epithelial cells (22) and is mainly expressed in differentiated epithelial cells, such as luminal cells of the prostate (23), we hypothesize that KLF5 maintains epithelial characteristics and represses EMT in epithelial cells.

EMT is a complicated but critical cellular process by which epithelial cells lose their epithelial characteristics and acquire a mesenchymal-like phenotype (12). The phenotypic changes in EMT include loss of cell-cell adhesion mediated by CDH1 downregulation and involve the acquisition of motile ability, the expression of several mesenchymal markers (such as FN1, CDH2, and ZEB1), and the concomitant reorganization of the cytoskeleton (24–26). The underlying mechanisms for EMT, however, are still not fully understood. Transforming growth factor β (TGF-β) is a major inducer of EMT in various tissues during development, tumorigenesis, and tissue wound repair (27, 28) and is frequently used to induce EMT in different cell culture models (26). In some epithelial cells, such as those of the HaCaT epidermal epithelial cell line, which express a high level of KLF5 (22), TGF-β alone is insufficient to induce EMT (29) and the addition of epidermal growth factor (EGF) is required (30).

EMT can be regulated by a number of molecules, one class of which are microRNAs (miRNAs) (31–37). miRNAs are noncoding small RNAs that usually silence or repress gene expression by targeting the 3′ untranslated regions (UTRs) of mRNAs. Notably, the miRNA 200 (miR-200) family has been shown to repress EMT by targeting ZEB1 and ZEB2, both of which transcriptionally repress CDH1 and cause alterations in the plasticity and motility of epithelial cells (32, 33, 38).

In this study, we tested whether and how KLF5 regulates EMT in epithelial cells. Using TGF-β- and EGF-treated epithelial cells as a model of EMT, we found that KLF5 was significantly downregulated during EMT and knockdown of *KLF5* also induced EMT regardless of TGF-β treatment. Ectopic expression of KLF5, on the other hand,

Received 20 June 2013 Returned for modification 2 August 2013
Accepted 7 October 2013
Published ahead of print 14 October 2013
Address correspondence to Jin-Tang Dong, j.dong@emory.edu.
Supplemental material for this article may be found at http://dx.doi.org/10.1128/MCB.00787-13.

doi:10.1128/MCB.00787-13

attenuated the EMT induced by TGF-β and EGF. Expression profiling and biochemical analyses indicate that KLF5 transcriptionally activates the miR-200 miRNA family to prevent the induction of EMT. Overexpression of the miR-200 family prevented EMT induced by either the knockdown of *KLF5* or treatment with TGF-β and EGF. Repression of the miR-200 family by *Klf5* knockout was also confirmed in mouse prostates. These findings indicate that KLF5 maintains epithelial characteristics and represses EMT via transcriptional activation of the miR-200 family.

MATERIALS AND METHODS

Cell lines and other materials. The HaCaT epidermal epithelial cell line was established by Norbert E. Fusenig of the German Cancer Research Center (39), and culture conditions were the same as those previously described (39). Cells of the MCF-10A, PZ-HPV-7, HepG2, and MDA-MB-231 cell lines were purchased from the American Type Culture Collection (ATCC; Manassas, VA) and propagated following ATCC's instructions, with the exception of MCF-10A cells, which were propagated as previously described (40). The TGF-β used in this study was TGF-β1, purchased from R&D Systems (Minneapolis, MN). EGF was from Sigma (Beijing, China). The sense sequence of small interfering RNA (siRNA) for KLF5 was 5′-AAGCUCACCUGAGGACUCAdTdT-3′, which was established in a previous study (41). Mimics for miR-200a and miR-200c (RiboBio, Guangzhou, Guangdong, China) were used to overexpress miR-200a/c in HaCaT cells, and nonspecific miRNA mimics (RiboBio) were used as the control.

Mouse strains and breeding and prostate tissue sample collection. *Klf5* floxed mice, generated at Ozgene in Australia, were crossed with the PB-Cre4 transgenic mouse strain as described in our previous study (23). *Pten* floxed mice (The Jackson Laboratory) were introduced to achieve the *Pten* knockout background in the prostate. Prostates from mice sacrificed at different time points (24 months for $Pten^{WT/WT}$ mice, 18 months for $Pten^{flox/WT}$ mice, and 4 or 6 months for $Pten^{flox/flox}$ mice) were freshly collected for RNA isolation or formalin fixation. For RNA isolation, anterior prostate tissue samples were used for both the *Pten* wild-type (WT) group and the *Pten* knockout group. Mice used in these studies were housed at the Division of Animal Resources (DAR) facility at Emory University and handled by DAR staff. All mice were closely monitored and humanely euthanized. All experimental procedures involving animals were approved by the Institutional Animal Care and Use Committee (IACUC protocol no. 2001137).

Plasmid construction. The PLHCX-KLF5 expression vector was constructed by PCR amplification of the coding region of *KLF5* with the PCR primers listed in Table S1 in the supplemental material, digestion with HindIII and ClaI, and subsequent cloning into the PLHCX plasmid (Clontech, Mountain View, CA). The two miR-200 promoters (38) were also cloned by PCR amplification using genomic DNA from MCF7 cells and the primers listed in Table S1 in the supplemental material. The promoter for the miR-200c/141 cluster was from positions −979 to +26 (1,005 bp), and that for the miR-200b,a/429 cluster was from positions −4613 to −3141 (1,473 bp). PCR products were digested with XhoI and HindIII for the miR-200c/141 promoter and KpnI and HindIII for the miR-200b,a/429 promoter and cloned into the pGL3 basic plasmid (Promega, Madison, WI). PCR-based cloning or annealing of synthesized oligonucleotides was used to generate truncations of promoter-reporter plasmids, and primer sequences are listed in Table S1 in the supplemental material. Four mutants with mutations in the KLF5 binding sites, three for the miR-200c/141 promoter and one for the miR-200b,a/429 promoter, were also constructed by PCR-based approaches with the primers listed in Table S1 in the supplemental material. All plasmids were sequenced to confirm their sequences.

Luciferase reporter assay. miR-200 promoter activity assays were carried out in HepG2 cells using 0.2 μg promoter plasmids. Cells were cotransfected with 0.4 μg (or the amount indicated) of the pcDNA3.1-KLF5 or pcDNA3.1 plasmid and 0.005 μg pGL4.70 (*Renilla* luciferase; Promega) as an internal control. The Lipofectamine 2000 reagent (Invitrogen) was used for plasmid transfections according to the manufacturer's instructions. Forty-eight hours after transfection, cells were lysed with 100 μl of passive lysis buffer (Promega), and luciferase activities were measured from 20 μl of cell lysates by using the dual-luciferase reporter assay on a Berthold FB12 luminometer (Berthold, Bad Wildbad, Germany). Firefly luciferase activities were normalized by the *Renilla* luciferase activities. Experiments were performed in triplicate.

Oligonucleotide pulldown assay. Oligonucleotides for the miR-200c/141 and miR-200b,a/429 promoters, with biotin added to the 5′ ends, were synthesized by Invitrogen (Beijing, China). The sequences for the oligonucleotides were as follows: pmiR-200c/141 WT, biotin-5′-AGGTGGGCGGGCTGGGCGG-3′; pmiR-200c/141 M3, biotin-5′-AGGTAAGTAGGCTGGGCGG-3′; pmiR-200c/141 M4, biotin-5′-AGGTGGGCGGGCTAAGTAG-3′; pmiR-200c/141 M3M4, biotin-5′-AGGTAAGTAGGCTAAGTAG-3′; pmiR-200b,a/429 WT, biotin-5′-GCCGGCCGAGCCCATGGGCGG-3′; and pmiR-200b,a/429 Mc, biotin-5′-GCCGGCCGAGCCCATAAGTAG-3′. Each pair of oligonucleotides was annealed following standard protocols. After culture for 48 h, HaCaT cells were harvested and measured as previously described (22).

ChIP assay. HepG2 cells were transfected with pcDNA3-FLAG-KLF5 (42) or pcDNA3-FLAG with the Lipofectamine 2000 reagent (Invitrogen). Twenty-four hours after transfection, cells were harvested, and a chromatin immunoprecipitation (ChIP) assay kit (Millipore) was used to perform the ChIP assay following the manufacturer's protocol. Precipitated DNA was subjected to PCR with primers for the miR-200c/141 promoter (5′-GCAGCAGGGCTCACCAGGAA-3′ and 5′-CCCAACCGCACCCAAACA-3′) and primers for the miR-200b,a/429 promoter (5′-CCCTTGGGCTCTGGAGTCTG-3′ and 5′-CTGTACCAGACCAGCCACGAC-3′). Primers for the GAPDH (glyceraldehyde-3-phosphate dehydrogenase) gene were used as the control (35).

Lentiviral and retroviral infection. Five PLKO.1 lentiviral vectors expressing short hairpin RNAs (shRNAs) targeting *KLF5* mRNA (NM_001730.2) were purchased from Sigma and were prepared and used following the lentiviral protocols described on the Addgene website (http://www.addgene.org/lentiviral/protocols-resources/). After testing their knockdown efficiency, two lentiviruses (TRCN0000013636 and TRCN0000013637, in this study named sh36 and sh37, respectively) were chosen for use in experiments. PLKO.1 empty vector (SHC001; Sigma) was used as the control. HaCaT cells infected with shRNA-expressing virus vectors were selected for more than 96 h in medium containing 1 μg/ml puromycin (Sigma). For MCF-10A and PZ-HPV-7 cells, medium containing 2 μg/ml puromycin was used for selection.

The retrovirus system used for ectopic expression of KLF5 in HaCaT cells included expression vector PLHCX into which the KLF5-coding region was cloned, the vesicular stomatitis virus G-glycoprotein envelope vector, and the *gal*/*pol* expression vector Ecopac. The three vectors were transfected into HEK293T cells by using the Fugene HD reagent (Roche, Mannheim, Germany) according to the manufacturer's instructions. Media containing viruses were harvested at 48 h and 72 h and filtered (pore size, 0.45 μm; Millipore, Beijing, China). After infection with these viruses, HaCaT cells were selected in a medium containing hygromycin B (400 μg/ml; Roche) for at least 8 days.

Regular RT-PCR and real-time qPCR. Total RNA was isolated from cells using the TRIzol reagent (Invitrogen, Carlsbad, CA), and the first-strand cDNA for mRNA and miRNA was synthesized from total RNA using a reverse transcription (RT) kit from Promega. Regular RT-PCR and real-time quantitative PCR (qPCR) were performed to detect EMT markers. The primers used for these analyses are listed in Table S2 in the supplemental material. The mRNA level of *KLF5* was detected either by regular RT-PCR, as previously described (43), or by real-time qPCR by using the primers listed in Table S2 in the supplemental material. Bulge-loop miRNA qPCR primer sets for mature miR-200a/b/c were purchased from RiboBio and used according to the manufacturer's instructions. PCR products for miR-200a/b/c were cloned into the pMD18-T vector

(TaKaRa, Tokyo, Japan) for sequencing. The SYBR green (TaKaRa) method was used with a Realplex real-time PCR detection system (Eppendorf, Beijing, China) to detect gene expression. Real-time qPCRs were performed in triplicate, and each experiment was repeated at least twice. Results presented in the figures were from a representative experiment, except for the results of assays for the detection of miR-200 members in mouse prostate tissues.

Western blotting. Western blotting was performed following previously established procedures (42). KLF5 antibody was generated and described in our previous study (42). The antibody for CDH1 was purchased from Cell Signaling (Danvers, MA), and those for FN1 and CDH2 were purchased from BD Biosciences (Beijing, China). The β-actin antibody was purchased from Sigma.

Immunofluorescence staining and microscopy. For KLF5, CDH1, and FN1 staining, cells were fixed in 4% paraformaldehyde for 30 min, permeabilized with 0.5% (vol/vol) Triton X-100 for 10 min, blocked with 2% bovine serum albumin (BSA) for 2 h at room temperature, and incubated with a specific antibody (KLF5, 1:200; CDH1, 1:200; FN1, 1:1,000) overnight at 4°C. After washing, cells were incubated with the secondary antibody conjugated with fluorescein isothiocyanate (FITC) or tetramethyl rhodamine isocyanate at a dilution of 1:1,000 for 2 h at room temperature. DAPI (4′,6-diamidino-2-phenylindole) was used to stain nuclei. For F-actin staining, cells were fixed with cold methanol for 5 min, blocked with 2% BSA for 2 h, and incubated with β-actin antibody (1:500; Sigma) overnight at 4°C. For CDH1 and vimentin staining in mouse prostate tissue specimens, formalin-fixed paraffin-embedded tissues were sectioned at 5 μm, deparaffinized, rehydrated in graded ethanol, subjected to antigen retrieval, and incubated first with 10% goat serum and then with antibody for CDH1 (1:200; Cell Signaling) or antibody for vimentin (1:100; Cell Signaling) overnight at 4°C. The tissue specimens were then incubated with the secondary antibody conjugated with FITC (anti-rabbit antibody, 1:1,000 dilution) at 37°C for 1 h. DAPI staining was then performed. Fluorescence images were taken with an Olympus Plan Fluorite 40× (numerical aperture [NA], 0.75) objective lens at ambient temperature using an upright microscope (DM4000B; Leica, Wetzlar, Germany) equipped with a charge-coupled-device camera (DFC490; Leica). Images were acquired with the Leica Application Suit computer program (v3.8; Leica). Cell morphology was examined with an inverted phase-contrast microscope (AX10; Zeiss, Jena, Germany) with 10× (NA, 0.25) or 20× (NA, 0.3) objective lenses at ambient temperature, and images were collected by using a charge-coupled-device camera (AxioCam MRm; Zeiss) with AxioVision software (Zeiss).

For each picture of CDH1 staining (in RGB [red, green, blue] format), the 256 levels for the green channel were adjusted by removing the top 5 levels (to eliminate noise) and the bottom 15 levels (to eliminate the staining background) using the Adobe Photoshop program (Adobe, San Jose, CA). Each adjusted photo was then subjected to analysis with the ImageJ program. Briefly, the channels were split, and the histogram (pixels at each level) for the green channel was calculated by the ImageJ program for each photo. The mean fluorescence intensity (MFI) of CDH1 for each photo was calculated by using the formula $C_{total} \times \text{mean}/(C_{total} - C_0)$, where C_{total} is the total number of pixels, mean is the average level per pixel, and C_0 is the number of pixels at level 0 (total, 256 levels). Six to 18 photos from 2 or 3 mice were used for CDH1 measurement.

For vimentin staining, the number of epithelial cells with a green signal (vimentin-positive cells) and the number of epithelial cells with a blue DAPI signal (total number of cells) were counted for each photo, and the percentage of vimentin-positive cells was calculated by dividing the former by the latter. At least six different photos (representing six different fields) from 2 to 3 mice were used for vimentin measurement.

Migration assay. HaCaT cells in medium with 1% fetal bovine serum (FBS) were seeded onto the upper chamber of a Transwell (8 μm; Millipore), and medium containing 10% FBS, 2 ng/ml TGF-β, and 100 ng/ml EGF was added into the lower chamber. After 16 h at 37°C in a humidified chamber supplemented with 5% CO_2 in air, Transwell membranes were fixed in 4% paraformaldehyde for 1 h. The cells on the upper surface of the membrane were scraped with a cotton swab, and the cells on the lower surface were stained with 0.1% crystal violet (Sigma) for 0.5 h. Cells were then eluted for 10 min in 250 μl of 10% acetic acid, and the absorbance was measured at 570 nm and divided by the absorbance of an equal number of seeded cells to indicate the migration rates. Each treatment was performed in triplicate, each experiment was repeated at least twice, and consistent results were obtained each time. The migration assays for MCF-10A and PZ-HPV-7 cells were the same as those for HaCaT cells, except that Dulbecco modified Eagle medium–F-12 medium containing horse serum was used for MCF-10A cells and the migration took place for 12 h and keratinocyte serum-free medium (KSFM) was used for PZ-HPV-7 cells and the migration took place for 48 h.

Statistical analysis. Readings in all experiments are expressed as means ± standard errors. The statistical significance of differences between two groups was determined by unpaired Student *t* test, and *P* values of 0.05 or smaller and 0.01 or smaller are indicated in the figure legends. In some figures, *P* values are noted on the panels.

RESULTS

KLF5 is significantly downregulated during the EMT process *in vitro*. In our previous studies, we found that the HaCaT epidermal epithelial cell line expresses a high level of KLF5, which is essential for TGF-β to inhibit the proliferation of these cells (22, 44, 45). TGF-β alone does not induce complete EMT in HaCaT cells (29). However, combined treatment with TGF-β and EGF induces EMT in HaCaT cells, which have been established as an *in vitro* model of EMT (30, 46). Considering that KLF5 is integral to TGF-β-Smad signaling in the regulation of epithelial proliferation, we hypothesized that KLF5 also plays a key role in EMT. Consistent with published findings (30, 46), treatment with TGF-β and EGF shifted the morphology of HaCaT cells from epithelial to fibroblast-like (Fig. 1A) and induced the expected molecular changes, which included the downregulation of the epithelial marker E cadherin (CDH1) and upregulation of the mesenchymal marker fibronectin (FN1) (Fig. 1B to F), occasional localization of CDH1 in the cytoplasm (Fig. 1F), and delocalization of F actin (Fig. 1F). These changes validated the model of EMT for this study. During the induction of EMT in this model, the expression of KLF5 was significantly reduced at the protein level, although an increase at the mRNA level was detected shortly after the treatments, as detected by regular RT-PCR and real-time qPCR for mRNA (Fig. 1B and C) and by Western blotting (Fig. 1D and E) and immunofluorescent (IF) staining (Fig. 1F) for protein. The downregulation of KLF5 was gradual and more than 50% at 36 and 48 h of treatment (Fig. 1E).

Another mesenchymal marker, ZEB1, which represses CDH1 expression, was induced at 12 h at the RNA level, but the expression gradually disappeared thereafter (Fig. 1B and C). However, ZEB1 protein was not detectable by Western blotting during the EMT. The expression of ZEB2 was hardly detectable in HaCaT cells even after treatment with TGF-β and EGF.

Whereas *KLF5* mRNA expression rapidly increased to almost 3-fold shortly after treatment with TGF-β and EGF and with longer treatment eventually decreased to the pretreatment level (Fig. 1C), the protein level of KLF5 did not show an increase after the same short treatment (Fig. 1B). Protein degradation indeed occurred even with a short treatment of TGF-β and EGF (Fig. 1G), as shown in the cycloheximide (CHX) chase assay, where the degradation of the KLF5 protein was faster in the group treated with TGF-β and EGF than in the control group (Fig. 1G). We also addressed whether the downregulation of KLF5 is caused by TGF-β, EGF, or a combination and found that both TGF-β and

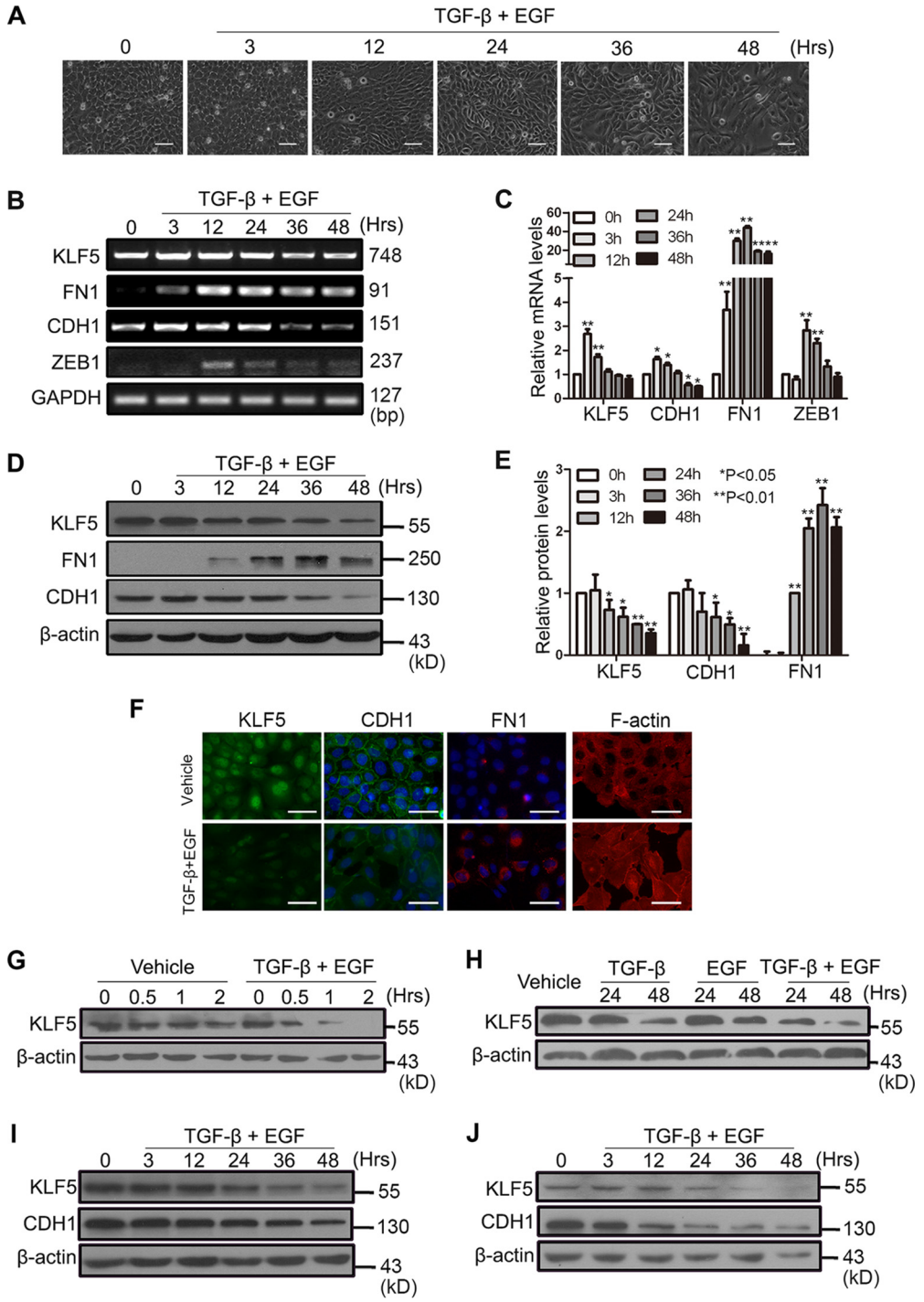

FIG 1 KLF5 is downregulated during the EMT induced by TGF-β and EGF in epithelial cells. (A) Phase-contrast images of HaCaT cells developing EMT after serum starvation (1% serum for 6 h) and TGF-β (2 ng/ml) and EGF (100 ng/ml) treatment for the indicated times. Magnification, ×200. (B to E) Expression of KLF5 and EMT markers CDH1, FN1, and ZEB1 during the induction of EMT, shown in panel A, as detected by RT-PCR (B), real-time qPCR (C), Western blotting (D), and the quantification of band intensities of Western blots (E). GAPDH and β-actin served as loading controls. Each experiment was repeated at least three times. Error bars represent the standard errors of the means. A *t* test of the results between the treatment and control groups was conducted. (F) Expression and cellular localization of KLF5 (green) and EMT markers CDH1 (green), FN1 (red), and F actin (red) in HaCaT cells treated with or without TGF-β (2 ng/ml) and EGF (100 ng/ml) for 48 h, as detected by IF staining. Bars, 50 μm. DAPI staining is also shown for CDH1 and FN1. (G and H) Detection of KLF5 and β-actin by Western blotting in HaCaT cells treated with cycloheximide (CHX; 50 μg/ml) and different combinations of TGF-β and EGF for different times. (I and J) Detection of KLF5, CDH1, and β-actin by Western blotting in MCF-10A cells (I; 10 ng/ml TGF-β and 100 ng/ml EGF) or primary mouse skin keratinocytes (J; 2 ng/ml TGF-β and 40 ng/ml EGF) for different times.

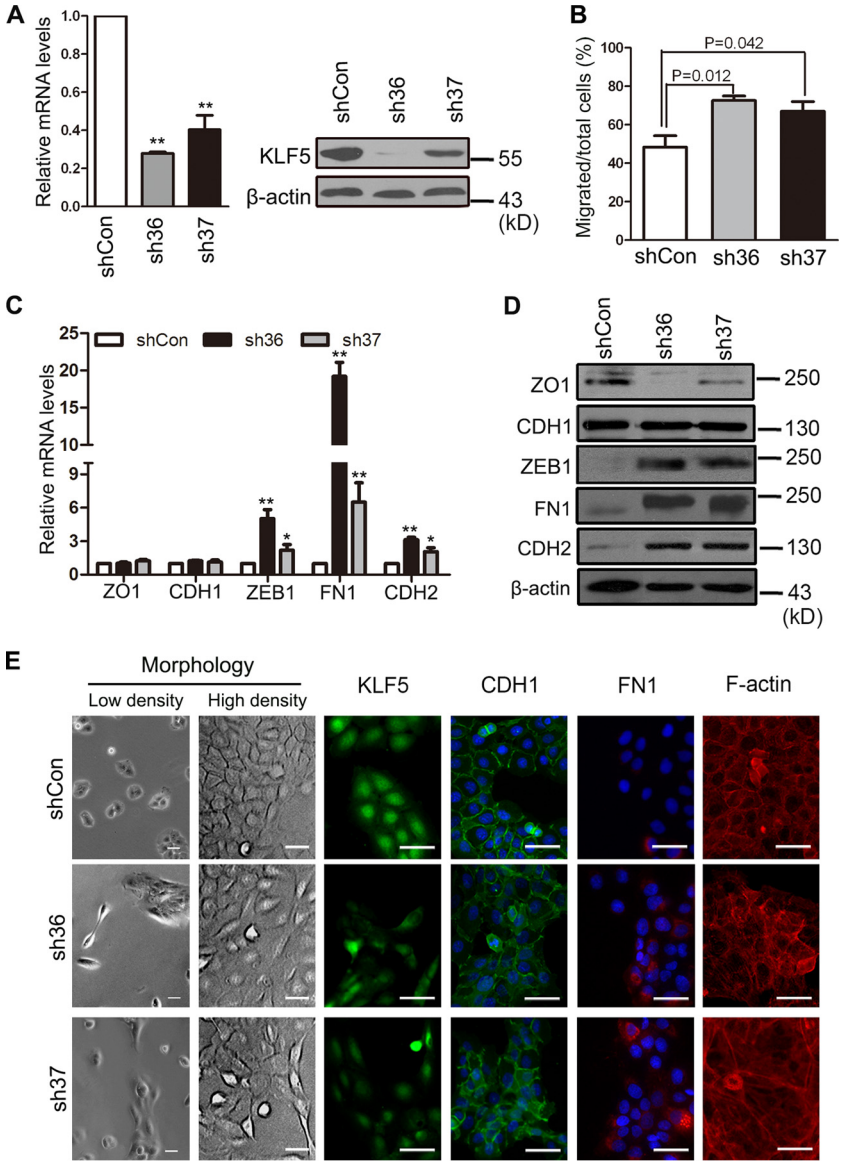

FIG 2 RNA interference-mediated silencing of *KLF5* induces EMT in HaCaT cells. (A) Confirmation of reduced KLF5 expression in HaCaT cells infected with lentiviruses expressing *KLF5* shRNA (sh36 and sh37, two different shRNAs) and control shRNA (shCon) by real-time qPCR (left) and Western blotting (right). (B) Silencing of *KLF5* increased the migration of HaCaT cells, as detected by Transwell assay with the cell populations from the experiments whose results are presented in panel A. The experiment was performed in triplicate, and error bars represent the standard errors of the means. (C to E) Silencing of *KLF5* induced the expression of mesenchymal markers ZEB1, FN1, and CDH2 and reduced the expression of epithelial marker ZO1, as detected by real-time qPCR (C) and Western blotting (D). (E) Cellular morphology was observed with a phase-contrast microscope (black-and-white images; magnification, ×200). The expression and cellular localization of markers were also determined by IF staining (color images; magnification, ×400). Bars, 50 μm. *, $P \leq 0.05$; **, $P \leq 0.01$.

EGF could reduce KLF5 protein separately and that combined treatment with TGF-β and EGF accelerated the effect (Fig. 1H). We asked if the KLF5 degradation is specific to HaCaT cells. In MCF-10A cells, cotreatment with TGF-β and EGF also reduced KLF5 at the protein level (Fig. 1I). In mouse primary keratinocytes, which we isolated as described previously (47), treatment with TGF-β also downregulated the KLF5 protein level (Fig. 1J). In these two additional cellular models, downregulation of KLF5 was also accompanied by downregulation of CDH1. These findings prove the downregulation of KLF5 during the EMT induced by TGF-β and EGF.

Knockdown of *KLF5* induces EMT in epithelial cells. Based on the significant downregulation of KLF5 during TGF-β- and EGF-induced EMT, we tested the hypothesis that the silencing of *KLF5* could play a causal role in EMT induction. We knocked down *KLF5* in HaCaT cells using lentiviruses expressing shRNAs against *KLF5*. Two of the shRNA-expressing viruses significantly knocked down *KLF5* expression, as verified at both the RNA and protein levels in stable cell populations (Fig. 2A). During the culture of these HaCaT-derived cells, silencing of *KLF5* made them easier to detach from the plates after trypsin treatment, which indicates a reduced epithelial morphology. To determine whether

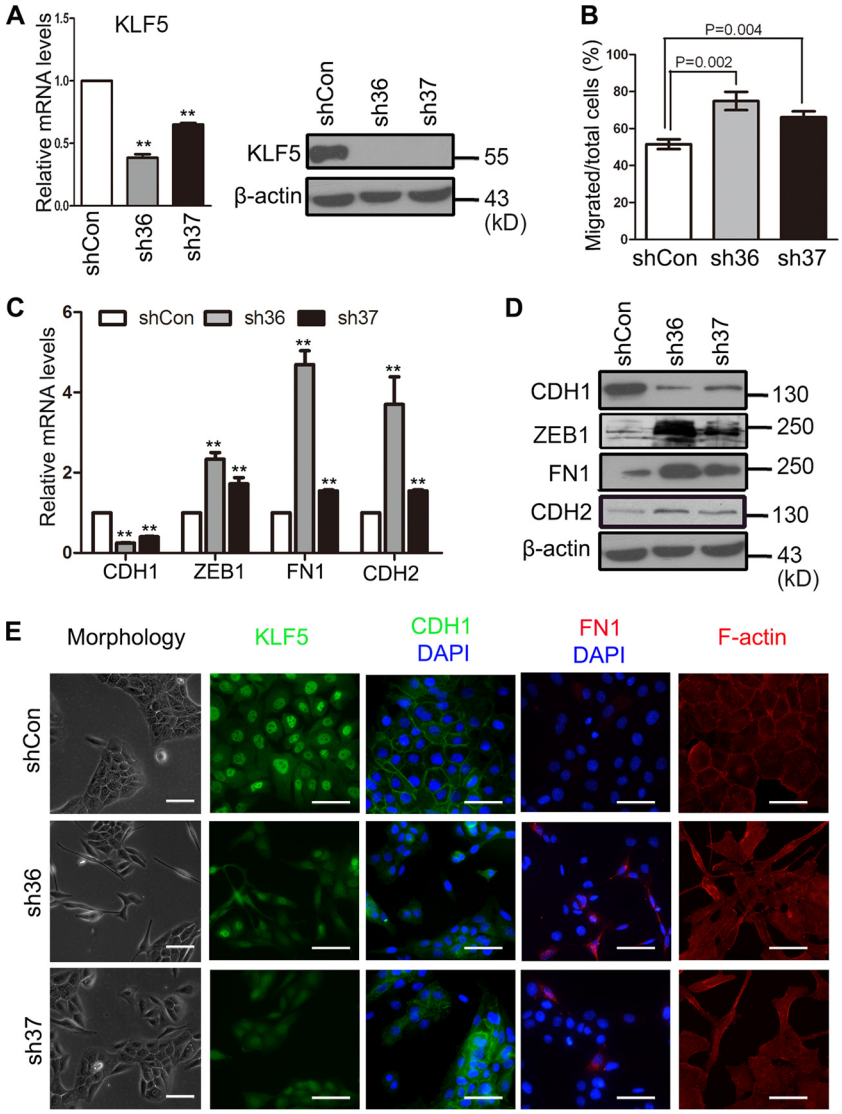

FIG 3 RNA interference-mediated knockdown of *KLF5* induces EMT in MCF-10A cells. (A) Confirmation of *KLF5* knockdown efficiency by shRNA expression by real-time qPCR assay (left) and Western blotting (right). sh36 and sh37 represent two different shRNAs targeting *KLF5*, whereas shCon is the shRNA control. (B) Knockdown of *KLF5* accelerates the migration of MCF-10A cells, as determined by Transwell assay. The experiment was performed in triplicate, and error bars represent the standard errors of the means. (C to E) Knockdown of *KLF5* upregulates EMT markers ZEB1, FN1, and CDH2 but downregulates EMT marker CDH1, as detected by real-time qPCR assay (C), Western blotting (D), and IF staining (E, colored panels; magnification, ×400; bars, 50 μm). (E, left) Cellular morphology was observed by use of a phase-contrast microscope. Magnification, ×200. **, $P \leq 0.01$.

KLF5 downregulation induces EMT, we first measured cell migration because an increase in cell migration is a common feature of EMT. Knockdown of *KLF5* indeed promoted the migration of HaCaT cells (Fig. 2B). We also evaluated the expression of EMT markers CDH1, ZO1, ZEB1, CDH2, and FN1. Real-time qPCR and Western blotting demonstrated the upregulation of mesenchymal markers ZEB1, CDH2, and FN1 and the downregulation of epithelial marker ZO1 after *KLF5* knockdown (Fig. 2C and D). Although the expression of epithelial marker CDH1 was not changed by *KLF5* knockdown, IF staining demonstrated that the membrane localization of CDH1 was disturbed by *KLF5* knockdown (Fig. 2E), indicating a loss of cell adhesion. IF staining also showed that *KLF5* knockdown increased FN1 expression in the cytoplasm and delocalized actin filaments (F actin) from the actin adhesion belt to linear bundles (a characteristic of mesenchymal cells) (Fig. 2E). Morphologically, a significant portion of cells (21% in one population and 32% in the other) retained a fibroblast-like phenotype even after the cells reached a high density (Fig. 2E). These results suggest that downregulation of KLF5 is necessary to induce EMT.

To further test the effect of *KLF5* knockdown on EMT, we also knocked down *KLF5* expression in two other immortalized but nontumorigenic epithelial cell lines, the MCF-10A mammary epithelial cell line and the PZ-HPV-7 prostate epithelial cell line (48, 49), and examined them for molecular and morphological changes. In both cell lines, *KLF5* knockdown also induced EMT, as indicated by an increase in cell migration (Fig. 3B; data not shown), downregulation of epithelial marker CDH1 and upregu-

TABLE 1 KLF5-regulated miRNAs that have been reported to be either EMT inhibitors or activators[a]

Regulation and miRNA	Expression change(s) upon *KLF5* knockdown
Downregulated	
miR-200a/200b/200c/141/429	0.59/0.6/0.6/0.59/0.59
miR-205	0.58
Let-7a/7b/7c/7d/7e/7g	0.57/0.59/0.28/0.57/0.55/0.6
miR-192	0.3
miR-203	0.29
miR-34b/34c	0.47/0.03
miR-30a-3p/30a-5p/30c/30d	0.47/0.49/0.59/0.25
miR-126	0.6
miR-365	0.29
miR-138	0.29
miR-15b	0.29
miR-125a	0.59
miR-23b	0.16
miR-149	0.29
miR-372	0.58
miR-31	0.59
miR-106b	0.6
Upregulated	
miR-155	2.37
miR-661	1.91

[a] A total of 756 miRNAs were screened for expression changes upon the knockdown of *KLF5* in HaCaT cells. Of the 756 miRNAs, 223 were downregulated (fold change ≤ 0.6), and 53 were upregulated (fold change ≥ 1.5). For each of the 223 downregulated and 53 upregulated miRNAs, the PubMed database was searched with the miRNA name and EMT as keywords, and the resultant publications were evaluated to determine whether an miRNA is an inhibitor or activator of EMT. The order of miRNAs listed in the table is based on the number of publications (the most at the top and the fewest at the bottom) available for these miRNAs.

lation of mesenchymal markers (CDH2, FN1, and ZEB1) (Fig. 3C and D; data not shown), and delocalization of CDH1 and F actin (Fig. 3E). These results further indicate a role of KLF5 downregulation in EMT induction.

KLF5 knockdown downregulates the EMT-inhibitory miR-200 family. KLF5 is a transcription factor, so we predicted that EMT induced by *KLF5* knockdown is mediated by key transcriptional targets of KLF5. Several microarray-based studies have identified a large number of protein-coding genes that are transcriptionally regulated by KLF5 (3, 50–52). Evaluation of these KLF5 target genes did not point to significant regulators of EMT. We then hypothesized that miRNAs, which usually have a more profound regulatory impact on different biological processes, could mediate the effect of *KLF5* knockdown on EMT. Therefore, we performed TaqMan real-time qPCR-based miRNA screening in HaCaT cells expressing control shRNA (HaCaT-shCon cells) and HaCaT cells expressing an shRNA targeting *KLF5* (HaCaT-sh36 cells) (Table 1; see Data set S1 in the supplemental material). Analyses of the screening data identified a large number of miRNAs that were either downregulated ($n = 223$) or upregulated ($n = 53$) by *KLF5* knockdown (Table 1; see Data set S1 in the supplemental material). Interestingly, 30 of the 223 downregulated miRNAs were shown or suggested to be suppressors of EMT in previous studies. Among them, the miR-200 family was particularly interesting, because all five members of this family were downregulated by *KLF5* knockdown (Table 1), and all had been shown to suppress EMT by targeting EMT inducers ZEB1 and ZEB2 (32–34). We therefore focused on the miR-200 family as key effectors of KLF5 in EMT regulation.

We further evaluated the expression of miR-200a/b/c by real-time qPCR in different cell lines with the knockdown of *KLF5*. Infection with viruses expressing *KLF5* shRNA or transfection of *KLF5* siRNAs downregulated each of these miRNAs in HaCaT cells (Fig. 4A). A similar effect was also detected in MCF-10A and PZ-HPV-7 cells infected with the viruses expressing KLF5 shRNA (Fig. 4B). We also transfected a KLF5-expressing plasmid into two cell lines, HepG2 and MDA-MB-231, which express little KLF5, and found that ectopic expression of KLF5 induced the expression of miR-200a/b/c (Fig. 4C), further supporting a regulatory relationship between KLF5 and the miR-200 family.

Members of the miR-200 family belong to two gene clusters, each with a distinct gene promoter (38). To further test the regulatory relationship between KLF5 and miR-200, we constructed a promoter-luciferase reporter plasmid for each cluster and cotransfected the plasmid with the KLF5 expression plasmid or a control into HepG2 cells. Ectopic expression of KLF5 induced significant luciferase activities for both the miR-200c/141 promoter and the miR-200b,a/429 promoter (Fig. 4D).

KLF5 directly regulates the miR-200 family by binding to the GC boxes of their promoters. As a transcription factor, KLF5 regulates its target genes by binding to the GC-rich sequences of promoters (8, 22). Sequence analysis of miR-200 promoters revealed four GC boxes (GGGCGG) in the miR-200c/141 promoter (Fig. 5A) and three in the miR-200b,a/429 promoter (Fig. 5B). To determine whether KLF5 binds to these GC boxes to directly regulate the miR-200 family, we first constructed a series of miR-200 promoter-luciferase constructs that contained different numbers of the GC boxes and tested their promoter activities (Fig. 5A and B). For the miR-200c/141 promoter, the −979, −690, and −407 promoter fragments, which had 4, 3, and 2 GC boxes, respectively, displayed similar strong activities in response to KLF5, indicating that the two proximal GC boxes have little impact on the promoter activity. However, deletion of the third GC box significantly reduced the promoter activity, and deletion of the fourth GC box eliminated the promoter activity (Fig. 5A), indicating that the third and fourth GC boxes (from positions −18 to −4) in the miR-200c/141 promoter are bound by KLF5 for regulation (Fig. 5A). Similarly, the third GC box in the miR-200b,a/429 promoter appeared to be essential for KLF5-induced promoter activity, whereas the other two GC boxes were dispensable (Fig. 5B).

We then generated mutant promoter-reporter plasmids in which one or both GC boxes in the miR-200c/141 promoter were interrupted to test if the GC boxes were necessary for KLF5-induced promoter activity. Mutation of both of the GC boxes but not each separately eliminated KLF5-induced activity in the miR-200c/141 promoter (Fig. 5C). In the miR-200b,a/429 promoter, mutation of the third GC box caused much less change in KLF5-induced promoter activity (Fig. 5D).

A ChIP assay was performed to further evaluate the binding of KLF5 to the GC boxes of the miR-200 promoters. Specific PCR products spanning the GC box region in both promoters were detected only in assays with FLAG-tagged KLF5-bound DNA and not in those with the negative controls (Fig. 5E). An oligonucleotide pulldown assay further confirmed the binding of KLF5 to the GC boxes, as the amount of KLF5 protein pulled down by biotin-labeled oligonucleotides spanning the GC boxes was significantly reduced when both GC

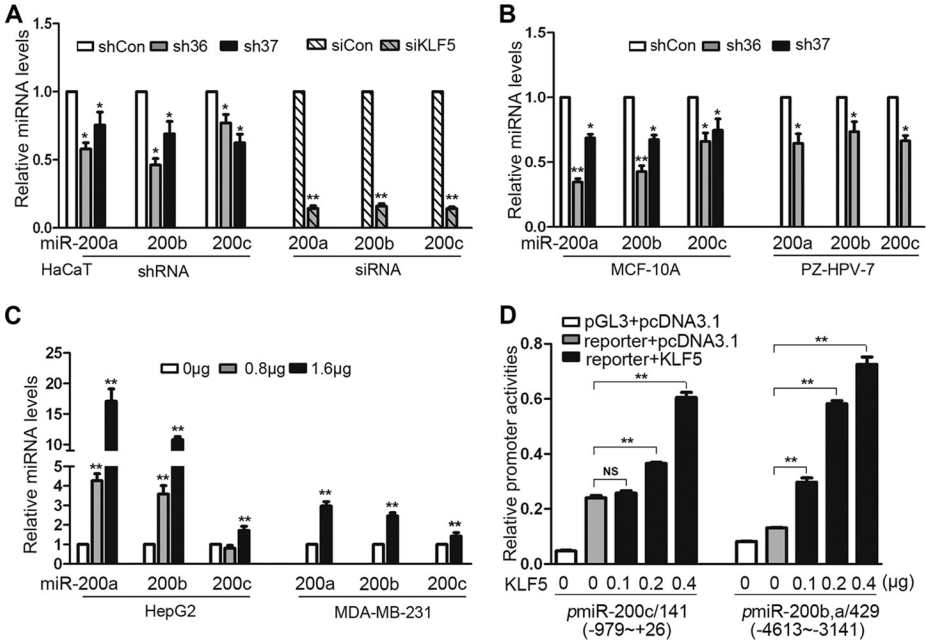

FIG 4 KLF5 induces the transcription of miR-200 members. (A and B) RNA interference-mediated knockdown of *KLF5* reduces the transcription of miR-200a/b/c in HaCaT (A), MCF-10A (B), and PZ-HPV-7 (B) cells, as determined by real-time qPCR. In addition to infecting cells with lentiviruses expressing shRNA against *KLF5* (sh36 and sh37) and control shRNA (shCon), chemically synthesized siRNA for *KLF5* (siKLF5) and control siRNA (siCon) were also transiently transfected into HaCaT cells (A, right). (C) Transfection of the KLF5 expression construct upregulates miR-200a/b/c in HepG2 and MDA-MB-231 cells, as detected by real-time qPCR. (D) Expression of KLF5 in HepG2 cells induces promoter activities for both the miR-200c/141 promoter (*p*miR-200c/141) and the miR-200b,a/429 promoter (*p*miR-200b,a/429), as measured by the luciferase activity assay. The experiment was performed in triplicate, and error bars represent the standard errors of the means. *, $P \leq 0.05$; **, $P \leq 0.01$; NS, not significant.

boxes in the miR-200c/141 promoter were mutated or when the third GC box in the miR-200b,a/429 promoter was mutated (Fig. 5F). These results indicate that KLF5 binds to the GC boxes of the miR-200 promoters to regulate their transcription.

Overexpression of miR-200 suppresses the EMT induced either by *KLF5* knockdown or by TGF-β and EGF treatment. The miR-200 family was demonstrated to suppress EMT in previous studies (33, 34, 53), so it is possible that downregulation of the miR-200 family via KLF5 downregulation plays a causative role in the EMT induced by *KLF5* knockdown. To test this prediction, we transfected mimics for miR-200a/c into HaCaT-sh36 cells, where KLF5 expression is knocked down by shRNA (Fig. 2A). Forced expression of miR-200a/c downregulated the mesenchymal markers ZEB1, FN1, and CDH2 even when *KLF5* was knocked down (Fig. 6A to C). Expression of miR-200a/c also restored the membrane localization of CDH1 and the adhesion belt localization of F actin and impaired the mesenchymal phenotype of HaCaT-sh36 cells (Fig. 6C). Functionally, forced expression of miR-200a/c abolished the acceleration of migration caused by *KLF5* silencing in HaCaT-sh36 cells (Fig. 6D). Similar experiments were also performed in MCF-10A cells, and consistent results were obtained (Fig. 6E to H). Therefore, restoration of miR-200 expression restores the epithelial characteristic of cells.

We further tested whether miR-200 can prevent the EMT induced by TGF-β and EGF treatment, which could clarify whether the KLF5–miR-200 axis plays a causal role in TGF-β- and EGF-induced EMT. We first analyzed the expression of miR-200 members during TGF-β- and EGF-induced EMT. A real-time qPCR assay demonstrated that the expression of miR-200a/b/c was significantly reduced by treatment with TGF-β and EGF in HaCaT cells (Fig. 7A), which is consistent with the effect of *KLF5* knockdown. Functionally, overexpression of miR-200 members by transfecting miR-200a and miR-200c mimics (Fig. 7B) into HaCaT cells downregulated the mesenchymal markers ZEB1 and FN1 and upregulated the CDH1 epithelial marker in the presence of TGF-β and EGF (Fig. 7C to E). Morphologically, miR-200 expression halted the fibroblast-like transition induced by TGF-β and EGF, which was accompanied by increased CDH1 localization on the cellular membrane and F-actin localization to the actin adhesion belt (Fig. 7E). Expression of the miR-200 family also lowered the rate of cell migration caused by TGF-β and EGF (Fig. 7F). These results suggest that upregulation of the miR-200 family suppresses the EMT induced by TGF-β and EGF.

KLF5 restoration rescues miR-200 expression to attenuate TGF-β- and EGF-induced EMT. To further evaluate whether downregulating the KLF5–miR-200 axis plays a causal role in TGF-β- and EGF-induced EMT, we overexpressed KLF5 in HaCaT cells while treating them with TGF-β and EGF and then tested the effects on miR-200 expression and the molecular and morphological characteristics of EMT. Endogenous KLF5 expression is high in HaCaT cells (22), but treatment with TGF-β and EGF downregulated KLF5 (Fig. 1D to F). Retrovirus-mediated infection, however, increased KLF5 expression and attenuated the downregulation of KLF5 by TGF-β and EGF, as confirmed by both Western blotting and real-time qPCR (Fig. 8A and C). Furthermore, KLF5 overexpression suppressed the EMT induced by TGF-β and EGF, as indicated by the prevention of FN1 and ZEB1 upregulation and CDH1 downregulation (Fig. 8C to E). Overexpression of KLF5 in TGF-β- and EGF-

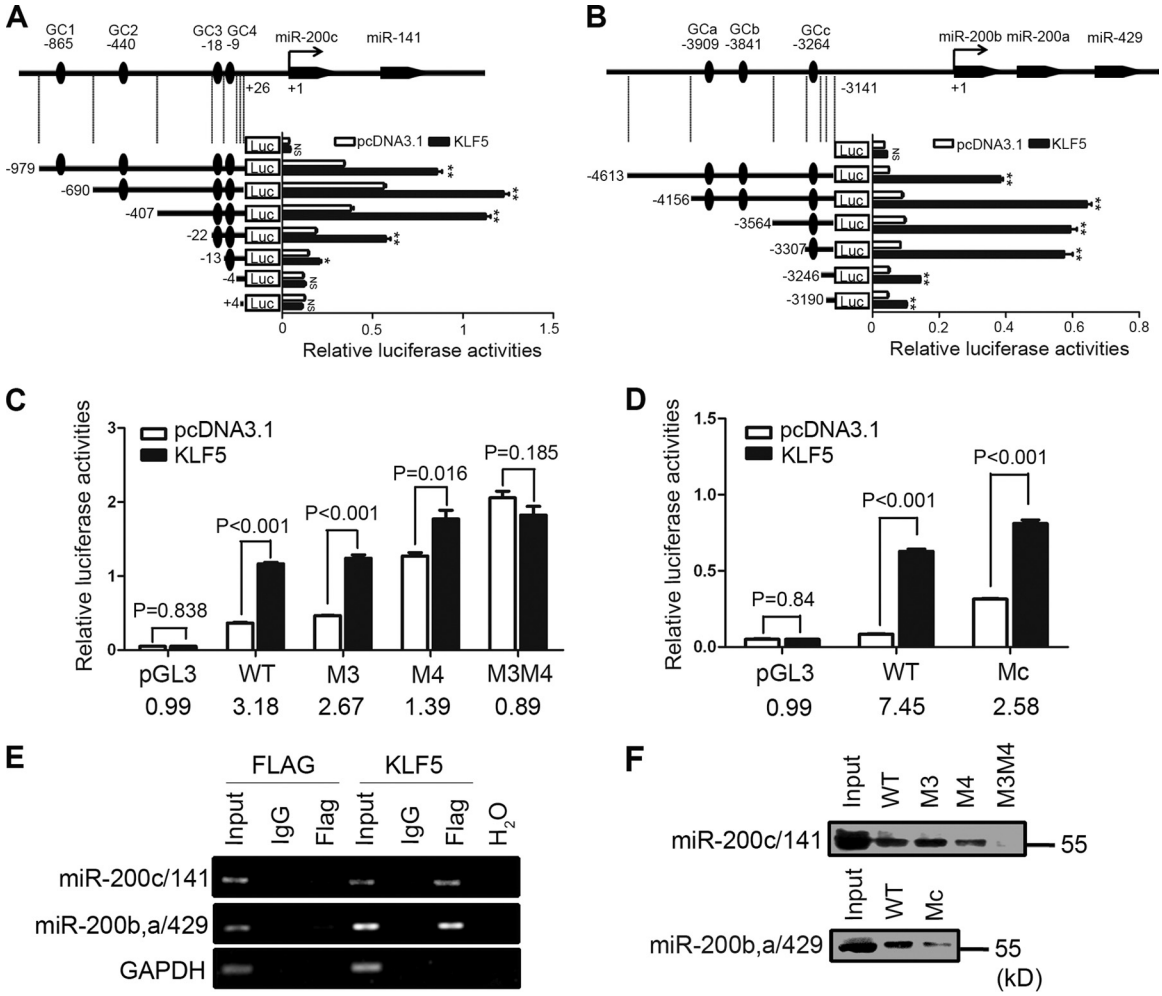

FIG 5 KLF5 upregulates miR-200 members by binding to GC boxes of their promoters. (A and B) Mapping of the promoter for miR-200c/141 (A) and that for miR-200b,a/429 (B) to search for their KLF5-responsive elements by the luciferase (Luc) promoter-reporter assay. Reporter plasmids with different sizes of promoter DNA were transfected with the expression plasmid for KLF5 or pcDNA3.1 as a control before the luciferase assay was conducted. The locations of GC boxes are marked by ovals. The first nucleotide of mature miR-200c (A) and miR-200b (B) in each cluster is indicated by +1. (C and D) Mutation of GC boxes (GGGCGG to AAGTAG) significantly compromises KLF5-induced transactivation activities for both the miR-200c/141 promoter (C) and the miR-200b,a/429 promoter (D). M3 and M4, mutation of the GC box at positions −18 and −9 (GC3 and GC4) of the miR-200c/141 promoter, respectively; Mc, mutation of the GC box at position −3264 (GCc) of the miR-200b,a/429 promoter. The fold change of KLF5-induced promoter activity for each construct is shown at the bottom. The experiment was performed in triplicate, and error bars represent the standard errors of the means. (E) Binding of KLF5 to the promoters of miR-200c/141 and miR-200b,a/429 detected by the ChIP-PCR assay. Specific PCR products spanned functional GC boxes on miR-200 family promoters. (F) Mutation of GC boxes abolishes the binding of KLF5 to the miR-200c/141 promoter, as determined by the oligonucleotide pulldown assay. Results are inclusive for the miR-200b,a/429 promoter. *, $P < 0.05$; **, $P \leq 0.01$; NS, not significant.

treated cells also enhanced localization to the actin adhesion belt (Fig. 8E) and reduced cell motility (Fig. 8F). Furthermore, KLF5 overexpression rescued the downregulation of miR-200 by TGF-β and EGF (Fig. 8B). These results suggest that maintaining a normal level of KLF5 expression interferes with the function of TGF-β and EGF in the induction of EMT by maintaining the expression of miR-200 members.

Knockout of *Klf5* in prostates of *Pten*-null mice promotes EMT characteristics. Although the results described above indicate a role for the KLF5–miR-200 axis in EMT, these results were from cultured cells, and thus, whether the axis also affects EMT characteristics *in vivo* is unknown. Previous studies indicated that KLF5 is ubiquitously expressed in epithelial cells of different tissues (8, 22), so we used mouse prostates, where knockout of *Klf5* significantly promotes the prostatic tumorigenesis induced by the knockout of *Pten* (C. Xing, X. Sun, X. Fu, Z. Zhang, X. Ci, R. D. Cardiff, and J. T. Dong, unpublished data). When *Klf5* was knocked out alone in the prostate, CDH1 expression showed little reduction, while no change in the expression of the mesenchymal marker vimentin was detectable (Fig. 9A). Among the miR-200 members, *Klf5* knockout significantly downregulated miR-200a and miR-200b but had no detectable effect on the expression of miR-200c (Fig. 9B, left). These findings suggest that although *Klf5* knockout has effects on the expression of miR-200 members, it is still insufficient to induce obvious EMT characteristics.

In the context of *Pten* knockout, *Klf5* knockout induced obvious EMT characteristics, including downregulation of CDH1, upregulation of vimentin, and the appearance of spindle-like cells

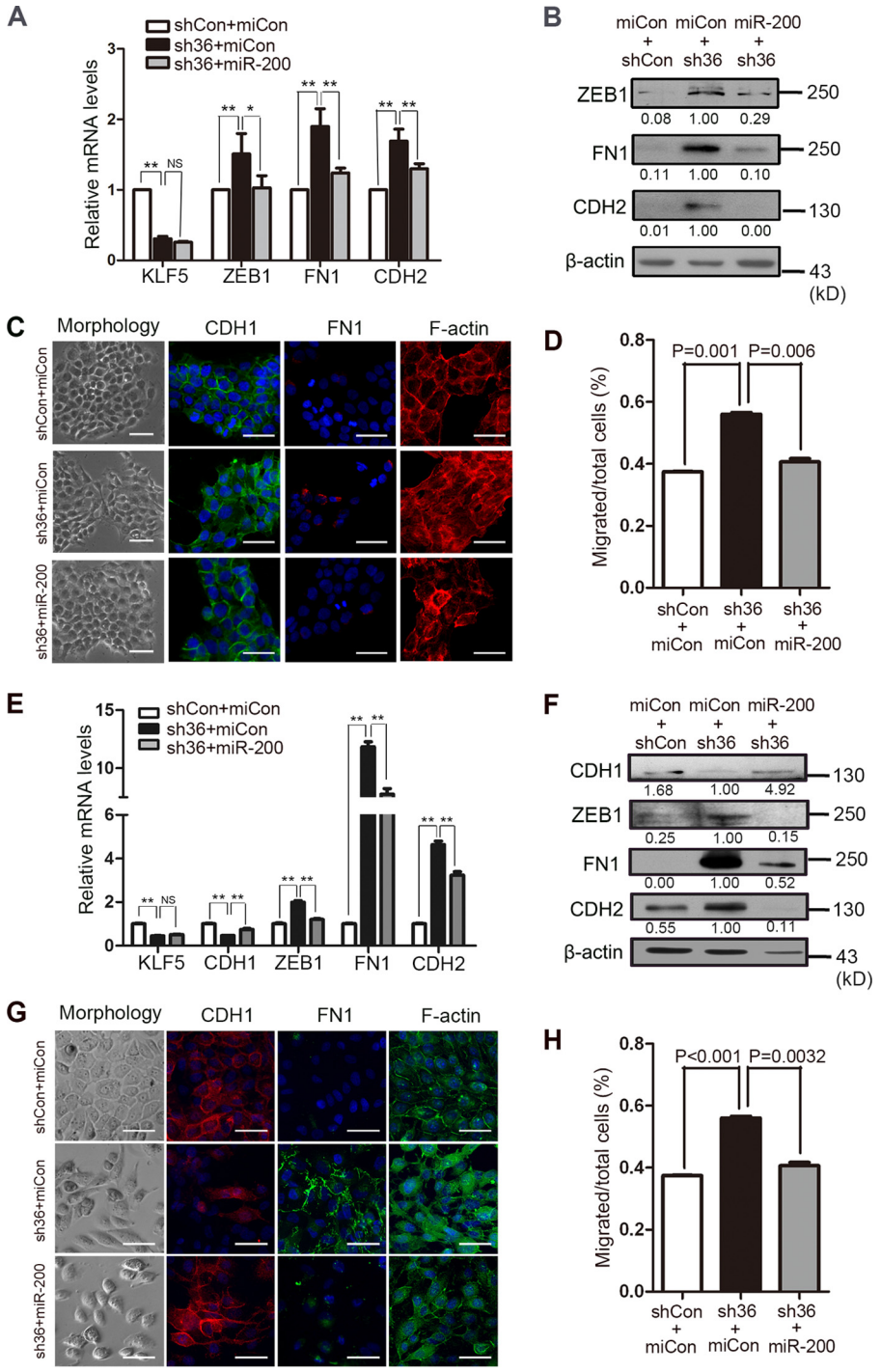

FIG 6 Downregulation of the miR-200 family rescues EMT induced by *KLF5* knockdown in both HaCaT and MCF-10A cells. (A, B, E, and F) Forced expression of miR-200a/c mimics attenuates the effect of *KLF5* silencing on the expression of CDH1, ZEB1, FN1, and CDH2, as determined by real-time qPCR (A and E) and Western blotting (B and F) in both HaCaT cells (A and B) and MCF-10A cells (E and F). Expression of *KLF5* was determined by real-time qPCR (A and E). (C and G) Forced expression of miR-200a/c mimics rescues the changes of cell morphology and EMT markers, including CDH1, FN1, and F actin, in HaCaT cells (C) and MCF-10A cells (G). (D and H) Overexpression of miR-200a/c suppresses the acceleration of migration caused by *KLF5* silencing in HaCaT cells (D) and MCF-10A cells (H), as determined by Transwell assay. The experiment was performed in triplicate, and error bars represent the standard errors of the means. The relative protein levels are marked under each lane. miCon, miRNA mimics control. Bars, 50 μm. *, $P \leq 0.05$; **, $P \leq 0.01$; NS, not significant.

(Fig. 9A). Meanwhile, the expression of miR-200a and miR-200b was significantly reduced (Fig. 9B, middle and right, respectively). These findings further indicate the role of the KLF5–miR-200 axis in EMT inhibition.

DISCUSSION

Whereas previous studies have suggested a role of KLF5 in EMT regulation (13, 15–19), cellular and molecular proofs are still lacking, and the underlying mechanisms are still unknown. In this

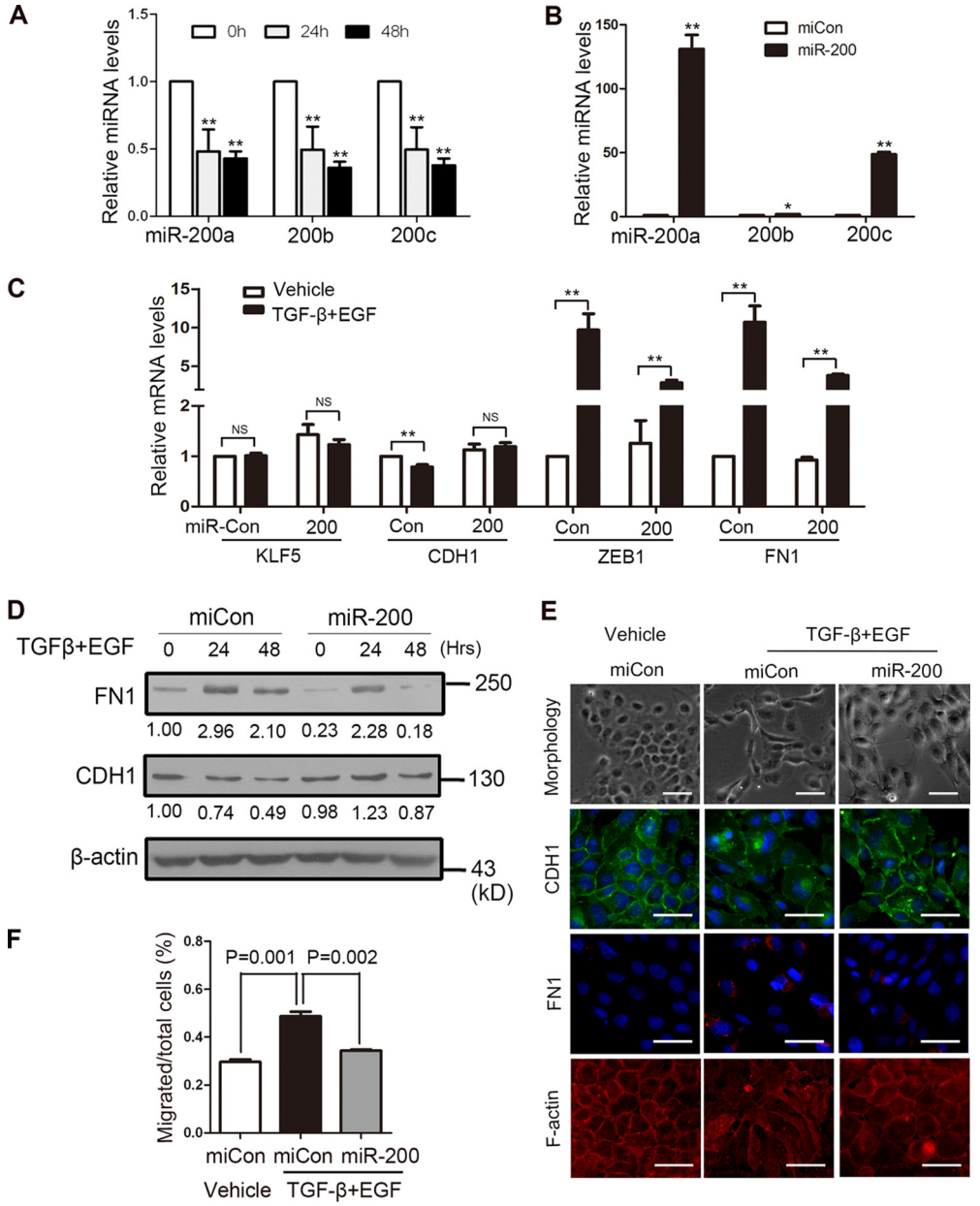

FIG 7 Downregulation of the miR-200 family plays a causative role in EMT induced by TGF-β and EGF. (A) Treatment with TGF-β (2 ng/ml) and EGF (100 ng/ml) for 24 h and 48 h downregulates miR-200a/b/c, as detected by real-time qPCR. (B) Confirmation of miR-200a/c overexpression by real-time qPCR after transfecting miR-200a/c mimics into HaCaT cells. (C and D) Forced expression of miR-200a/c mimics attenuates the effect of TGF-β (2 ng/ml) plus EGF (100 ng/ml) (24 or 48 h) on the expression of KLF5, CDH1, FN1, and ZEB1, as detected by real-time qPCR (C) and Western blotting (D). The relative protein levels, which are the ratios of proteins to β-actin in band intensities normalized by the control group, are marked under each lane in panel D. (E) Forced expression of miR-200a/c mimics rescues the morphology of the cells and the expression and locations of EMT markers, inclusive of CDH1, FN1, and F actin, which are disturbed by TGF-β plus EGF treatment in HaCaT cells, as detected by IF staining. (F) The migration induced by TGF-β plus EGF treatment was impaired by miR-200a/c overexpression, as determined by Transwell assay. The experiment was performed in triplicate, and error bars represent the standard errors of the means. The relative protein levels are marked under each lane. Bars, 50 μm. *, $P \leq 0.05$; **, $P \leq 0.01$; NS, not significant.

study, we examined the role of KLF5 in the maintenance of epithelial characteristics and the prevention of EMT induced by TGF-β and EGF, as well as how KLF5 executes such functions (Fig. 10). We found that KLF5 is necessary for the maintenance of the epithelial phenotype and molecular features and that downregulation of KLF5 is necessary for TGF-β and EGF to induce EMT in epithelial cells. We further identified, for the first time, the KLF5–miR-200 axis to be a mechanism for EMT regulation. The novel KLF5–miR-200 axis could play a role in multiple pathological and physiological processes.

KLF5 maintains epithelial characteristics via transcriptional activation of the miR-200 family. KLF5 was originally suggested to be an epithelial factor because of its ubiquitous expression in epithelial cells as well as its function in epithelial differentiation

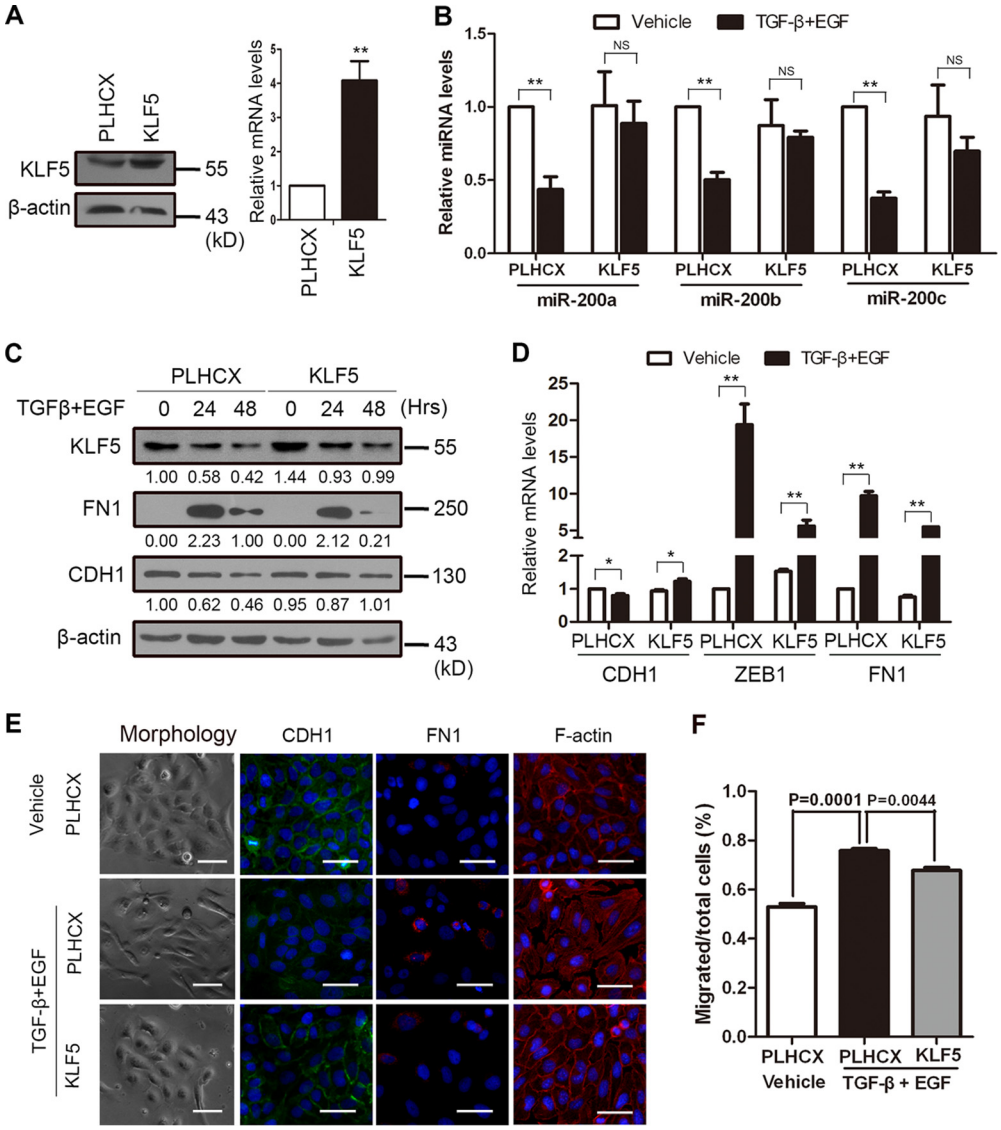

FIG 8 Ectopic expression of KLF5 interferes with TGF-β and EGF induction of EMT by rescuing miR-200 expression. (A) Confirmation of ectopic expression of KLF5 mediated by the PLHCX retroviral system by real-time qPCR (right) and Western blotting (left). (B) Ectopic expression of KLF5 rescues the downregulation of miR-200a/b/c induced by TGF-β plus EGF treatment in HaCaT cells, as determined by real-time qPCR. (C to E) Ectopic expression of KLF5 interferes with the expression of EMT markers in HaCaT cells treated with TGF-β (2 ng/ml) and EGF (100 ng/ml) for 24 or 48 h, as determined by Western blotting (C), real-time qPCR (D), and IF staining (E). The relative protein levels, which are the ratios of proteins to β-actin in band intensities normalized by the control group, are marked under each lane in panel C. Bars, 50 μm. (F) The migration ability enhanced by EMT induction was attenuated by ectopic KLF5 expression, as detected by Transwell assay. The experiment was performed in triplicate, and error bars represent the standard errors of the means. *, $P \leq 0.05$; **, $P \leq 0.01$; NS, not significant.

and the inhibition of cell proliferation (8, 22). Findings from our current study provide more direct evidence for the function of KLF5 as an epithelial factor. First, not only is KLF5 downregulated during the EMT induced by TGF-β and EGF, but also knockdown of *KLF5* alone induced the phenotypic and molecular characteristics of EMT, including a spindle-like cell shape, dislocation of the epithelial marker E cadherin and actin filaments, upregulation of the mesenchymal markers fibronectin and ZEB1, and enhanced cell migration (Figs. 1 to 3; data not shown). Although *KLF5* silencing failed to reduce the expression of CDH1 in HaCaT cells, it succeeded in two other cell lines: MCF-10A and PZ-HPV-7. In addition, silencing of *KLF5* in HaCaT cells caused the dislocation of CDH1 from the cellular membrane to the cytosol, which is also an indicator of EMT. Second, ectopic expression of KLF5 prevented the induction of EMT by TGF-β and EGF (Fig. 8). These results indicate that KLF5 is necessary for the maintenance of epithelial characteristics.

Establishment of the KLF5–miR-200 axis also supports the conclusion that KLF5 is a necessary epithelial factor. In searching for miRNAs that mediate the function of KLF5 in epithelial maintenance, we found that miR-200 members were also downregulated when KLF5 was downregulated. Functional and biochemical analyses further established a direct transcriptional regulatory relationship between KLF5 and the miR-200 family. In addition,

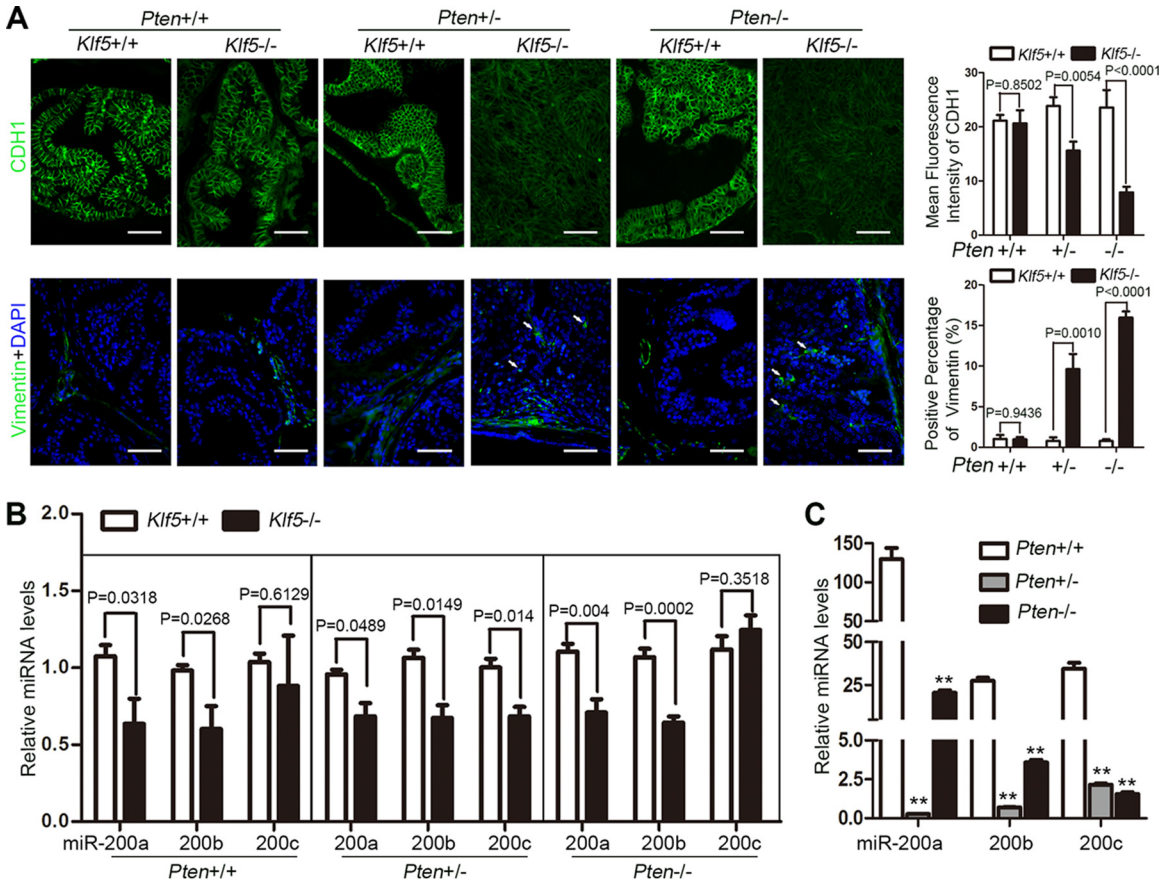

FIG 9 Knockout of *Klf5* downregulates the miR-200 family and induces EMT characteristics in the context of *Pten* deletion in mouse prostates. (A) Downregulation of CDH1 and upregulation of vimentin by *Klf5* deficiency in mouse prostates with *Pten* deletion, as detected by IF staining. Arrows, vimentin signals in the luminal epithelial cells of the prostate. At least six fields from two or three mice were used for calculating the mean fluorescence intensity of CDH1 and the percentage of vimentin-positive cells (summarized and shown on the right). Bars, 50 μm. (B) Downregulation of the miR-200 family by *Klf5* deficiency in mouse prostates with *Pten* deletion, as detected by real-time qPCR. *P* values are for differences between *Klf5* wild-type and *Klf5*-null groups. (C) Downregulation of miR-200 members by *Pten* knockout in mouse prostates with wild-type *Klf5*, as detected by real-time qPCR. The results are expressed as the means ± standard errors for three or more mice. **, $P \leq 0.01$.

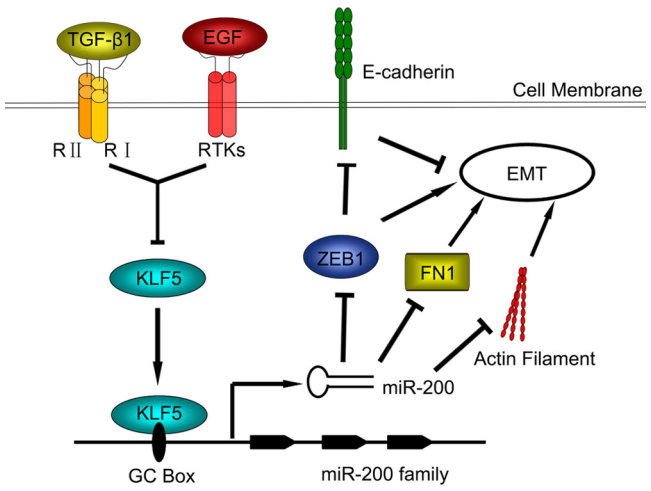

FIG 10 Model of how KLF5 regulates EMT in epithelial cells. The downregulation of KLF5 by TGF-β and EGF (or other factors) leads to the downregulation of miR-200 members, which subsequently dysregulates molecules underlying EMT, including the downregulation of CDH1 and upregulation of FN1 and ZEB1. RI, TGF-β type I receptor; RII, TGF-β type II receptor; RTKs, tyrosine kinase receptors.

ectopic restoration of miR-200 expression prevented the induction of EMT by TGF-β and EGF or by the knockdown of *KLF5* (Figs. 6 and 7), further establishing that miR-200 members are functional mediators of KLF5 in the maintenance of epithelial characteristics and EMT inhibition.

In mouse prostate tissues, a regulatory relationship between Klf5 and miR-200 was also detected (Fig. 9). Whereas knockout of *Klf5* decreased the expression of miR-200a/b regardless of *Pten* knockout status, which is consistent with the *in vitro* findings, the relationship between Klf5 and miR-200c was detectable only in *Pten* heterozygous mice and not in wild-type or *Pten* homozygous mice (Fig. 9B). It is possible that miR-200c is less responsive to *Klf5* knockout than miR-200a/b, because miR-200c also showed weaker responses to KLF5 overexpression in MDA-MB-231 and HepG2 cells (Fig. 4C). The miR-200b, a/429 cluster is located at the same locus on chromosome 1, while the miR-200c/141 cluster is at another locus on chromosome 12. The difference in gene promoters could thus be responsible for the difference in miR-200 transcription upon *Klf5* knockout. In addition, *Pten* knockout appeared to have a greater effect on the expression of miR-200 in mouse prostates (Fig. 9C), and knockout of one *Pten* allele had a much greater effect than the knockout of both *Pten* alleles for

miR-200a/b expression but not for miR-200c expression (Fig. 9C). The different effects of *Pten* knockouts on miR-200 expression could also affect the responses of miR-200a/b and miR-200c to *Klf5* knockout. These results further suggest that PTEN also regulates the expression of miR-200 members and EMT, which warrants further investigation.

A number of studies have established an important physiological role for the miR-200 family in the determination of epithelial differentiation during embryonic development and in the maintenance of the epithelial phenotype (54). For example, during the differentiation of differentiating embryonic stem cells (ESCs), which express the miR-200 family, maintenance of miR-200 expression prevents EMT and stalls differentiating ESCs at the epiblast-like stem cell stage (55). In addition, overexpression of miR-200 members can induce mesenchymal-epithelial transition in both cancer cells and fibroblasts (56–58). Furthermore, it has been well established that the miR-200 family targets ZEB1 and ZEB2, while ZEB1 and ZEB2 transcriptionally downregulate the miR-200 family, forming a double-negative feedback loop in the regulation of EMT (32–34, 38, 59). Taken together with our findings, we conclude that the KLF5–miR-200 axis is essential for the maintenance of epithelial characteristics by epithelial cells.

Downregulation of the KLF5–miR-200 axis is necessary for EMT induction. EMT is an important process that occurs during normal tissue development, tissue repair, and tumor development and progression. How EMT is regulated at the molecular level has been an important area of investigation. A number of studies have established TGF-β to be a driving factor in the induction of EMT (60–63). One major mechanism by which TGF-β induces EMT is to downregulate the expression of miR-200 members in a Smad-dependent manner, which leads to the upregulation of EMT inducers ZEB1 and ZEB2 and, subsequently, EMT (64–67). In fact, manipulation of the ZEB/miR-200 balance is able to switch cells between the epithelial and mesenchymal states (64). In this study, we found that KLF5 was downregulated during TGF-β- and EGF-induced EMT, that restoration of KLF5 expression prevented the downregulation of miR-200 members and the induction of EMT by TGF-β and EGF, and that KLF5 directly activated the transcription of miR-200 members (Figs. 1, 4, 5, and 8). Our findings indicate that KLF5 is a suppressor of EMT and that downregulation of KLF5 is necessary for TGF-β to induce EMT.

Transcriptional regulation of the miR-200 family by different factors during EMT. In addition to direct transcriptional repression by the ZEB1/2 transcription factors (68), the transcription of miR-200 members also involves multiple other factors. Similar to the effect of ZEB1/2 on miR-200 transcription, GATA3 is another transcriptional repressor of miR-200 members (69). Tumor suppressors p53 and RB, as well as two members of the p53 family, p73 and p63, transcriptionally activate the miR-200 family to suppress EMT and EMT-associated stem cell properties (35, 48, 70, 71). Perhaps more relevant to the role of KLF5 in miR-200 regulation is that Smad3 has also been shown to transcriptionally activate the miR-200 family by direct promoter binding (72). In our previous studies, we found that KLF5, Smad2-4, and the p300 acetylase form a transcriptional complex to acetylate KLF5 and regulate cell cycle genes in the inhibition of epithelial cell proliferation (22, 44, 45). It is thus possible, though yet to be confirmed, that the same KLF5-Smads-p300 complex is responsible for the activation of miR-200 members in epithelial cells.

ZEB1 and ZEB2, both of which are well-established transcriptional repressors of miR-200 members, also interact with Smads to mediate the downregulation of miR-200. In fact, ZEB2 was originally identified as Smad-interacting protein 1 (SIP1) (73). Interestingly, the p300 acetylase and its associated protein, PCAF, form a transcriptional complex with ZEB1 to cause the acetylation of ZEB1 and the subsequent release of miR-200 transcription (74). It thus appears that the KLF5-Smads-p300 association activates, while the ZEB1/2-Smads-p300 association inactivates, the transcription of miR-200. One outstanding question is whether KLF5 and ZEB1/2 interact in the transcriptional regulation of miR-200. For example, they could physically interact or compete in the interaction with Smads, p300, and other factors to execute opposite functions in miR-200 regulation.

Could the KLF5–miR-200 axis regulate other biological processes? Likely associated with its function in EMT regulation, the miR-200 family has been shown to modulate multiple pathological and physiological processes, including tumorigenesis, stem-like features of cancer cells, and the induction and maintenance of pluripotency. miR-200 members target multiple stem cell factors, such as Sox2, Klf4, Nanog, Oct4, and Lin28B (75, 76), and inhibit the characteristics of stem-like cancer cells, including the $CD133^+$ side population, sphere formation capacity, *in vivo* tumorigenicity in nude mice, and stem cell marker expression (77–79). During the reprogramming of fibroblasts to induced pluripotent stem cells (iPSCs) by exogenous transcription factors Oct4, Sox2, Klf4, and Myc, the mesenchymal-epithelial transition (MET), which is an early event in reprogramming fibroblasts to iPSCs, occurs, and miR-200 members are transcriptionally induced and functionally necessary for iPSC generation (57, 58). On the other hand, KLF5 suppresses tumorigenesis in prostate cancer (80). Klf5 compensates for Klf4 during the reprogramming of somatic cells into iPSCs (81, 82), is essential for normal self-renewal of mouse ESCs (83–85), and regulates lineage formation in preimplantation mouse embryos (86). It is possible, though yet to be clarified, that KLF5 and the miR-200 family function together, as established in this study, to regulate iPSC generation, stem cell renewal and maintenance, tumorigenesis, and development.

Could the role of KLF5 in EMT be context dependent? Cell migration is a functional indicator of EMT (26). Opposite the inhibition of cell migration by KLF5 in HaCaT cells observed in this study (Figs. 2B, 3B, and 8F), KLF5 could also promote cell migration in other cell types (6, 9, 10), including mouse primary esophageal keratinocytes, where *Klf5* appears to promote cell migration by inducing the expression of integrin-linked kinase (ILK) (10); bronchial smooth muscle cells, where interleukin-8-induced cell migration could be blocked by the knockdown of *KLF5* (9); and intestinal epithelial cells, where deletion of *Klf5* impairs the migration of Paneth cells (6). Therefore, it is possible that the role of KLF5 in EMT is context dependent.

An earlier study suggested that EMT and the invasiveness induced by *KLF5* knockdown depend on the mutation or ablation of p53 in esophageal squamous cell carcinoma (11). In HaCaT cells, both alleles of *p53* are mutated, which extends the p53 half-life and disrupts its DNA binding activity (87). Induction of EMT by *KLF5* silencing (Fig. 2) in HaCaT cells is thus consistent with the findings in esophageal cells, supporting a role of p53 mutation in EMT induction. In MCF-10A cells, both p53 alleles are wild type (88), yet *KLF5* silencing also induced EMT (Fig. 3). Whereas the epidermal HaCaT cell line is squamous, the mammary gland-originated MCF-10A line is not, which could be responsible for EMT

induction in cells with wild-type p53. In addition, insulin is necessary for the culture of MCF-10A cells but not for that of HaCaT cells, which could also contribute to the disparity. Whether the EMT induced by *KLF5* silencing is truly independent of p53 mutation status remains to be determined.

Previous studies have demonstrated that KLF5 also has opposite functions in both cell proliferation and tumorigenesis (5, 22, 44, 45, 50). The acetylation state of KLF5, which could be determined by the balance between tumor-suppressive and tumor-promoting signaling (22, 44, 45; X. Li, B. Zhang, R. Zhao, S. Xia, G. Ma, Q. Zhao, L. Fu, Z. Zhu, and J. T. Dong, unpublished data), has been shown to be responsible for the opposite functions of KLF5 in cell proliferation and tumorigenesis, with acetylated KLF5 being suppressive and unacetylated KLF5 being promoting. Such a context-dependent function of KLF5 could also be responsible for the observed opposite functions of KLF5 in cell migration control and EMT regulation. For example, acetylated KLF5 could suppress, while unacetylated KLF5 could promote, cell migration and EMT. This possibility is worth testing.

In summary, we found that the KLF5 protein was downregulated during the EMT induced by TGF-β and EGF in epithelial cells, that downregulation of KLF5 alone also caused EMT, that KLF5 activated miR-200 expression by directly binding to the GC boxes in the promoters of miR-200 members, and downregulation of KLF5 caused the downregulation of miR-200 members (Fig. 10). Downregulation of the miR-200 family, in turn, altered the expression of EMT markers, such as CDH1, CDH2, FN1, and ZEB1, reorganized actin filaments, promoted cellular migration, and made cells spindle-like (Fig. 10). These findings not only established a direct regulatory relationship between KLF5 and the miR-200 family, but they also revealed one key step during the EMT induced by TGF-β and EGF. The KLF5–miR-200 axis could modulate multiple pathological and physiological processes by regulating cellular EMT-MET plasticity, including cell migration, stemness, iPSC generation, tumorigenesis and metastasis, and development.

ACKNOWLEDGMENTS

We thank Peng Guo of the Xi'an Jiaotong University School of Medicine for advice, Yuanli Chen and Yunfan Yang of Nankai University for their comments on the manuscript and technological assistance during this study, and Lori King and Frederick Dong for editing the manuscript.

This work was supported by grant 81130044 from the National Natural Science Foundation of China and grant R01CA171189 from the National Cancer Institute, National Institutes of Health.

REFERENCES

1. **Shi H, Zhang Z, Wang X, Liu S, Teng CT.** 1999. Isolation and characterization of a gene encoding human Kruppel-like factor 5 (IKLF): binding to the CAAT/GT box of the mouse lactoferrin gene promoter. Nucleic Acids Res. **27:**4807–4815.
2. **Sur I, Unden AB, Toftgard R.** 2002. Human Kruppel-like factor5/KLF5: synergy with NF-kappaB/Rel factors and expression in human skin and hair follicles. Eur. J. Cell Biol. **81:**323–334.
3. **Wan H, Luo F, Wert SE, Zhang L, Xu Y, Ikegami M, Maeda Y, Bell SM, Whitsett JA.** 2008. Kruppel-like factor 5 is required for perinatal lung morphogenesis and function. Development **135:**2563–2572.
4. **Chen C, Bhalala HV, Vessella RL, Dong JT.** 2003. KLF5 is frequently deleted and down-regulated but rarely mutated in prostate cancer. Prostate **55:**81–88.
5. **Zheng HQ, Zhou Z, Huang J, Chaudhury L, Dong JT, Chen C.** 2009. Kruppel-like factor 5 promotes breast cell proliferation partially through upregulating the transcription of fibroblast growth factor binding protein 1. Oncogene **28:**3702–3713.
6. **McConnell BB, Kim SS, Yu K, Ghaleb AM, Takeda N, Manabe I, Nusrat A, Nagai R, Yang VW.** 2011. Kruppel-like factor 5 is important for maintenance of crypt architecture and barrier function in mouse intestine. Gastroenterology **141:**1302–1313.
7. **Bateman NW, Tan D, Pestell RG, Black JD, Black AR.** 2004. Intestinal tumor progression is associated with altered function of KLF5. J. Biol. Chem. **279:**12093–12101.
8. **Dong JT, Chen C.** 2009. Essential role of KLF5 transcription factor in cell proliferation and differentiation and its implications for human diseases. Cell. Mol. Life Sci. **66:**2691–2706.
9. **Kuo PL, Hsu YL, Huang MS, Chiang SL, Ko YC.** 2011. Bronchial epithelium-derived IL-8 and RANTES increased bronchial smooth muscle cell migration and proliferation by Kruppel-like factor 5 in areca nut-mediated airway remodeling. Toxicol. Sci. **121:**177–190.
10. **Yang Y, Tetreault MP, Yermolina YA, Goldstein BG, Katz JP.** 2008. Kruppel-like factor 5 controls keratinocyte migration via the integrin-linked kinase. J. Biol. Chem. **283:**18812–18820.
11. **Yang Y, Nakagawa H, Tetreault MP, Billig J, Victor N, Goyal A, Sepulveda AR, Katz JP.** 2011. Loss of transcription factor KLF5 in the context of p53 ablation drives invasive progression of human squamous cell cancer. Cancer Res. **71:**6475–6484.
12. **Thiery JP, Acloque H, Huang RY, Nieto MA.** 2009. Epithelial-mesenchymal transitions in development and disease. Cell **139:**871–890.
13. **Shimamura T, Imoto S, Shimada Y, Hosono Y, Niida A, Nagasaki M, Yamaguchi R, Takahashi T, Miyano S.** 2011. A novel network profiling analysis reveals system changes in epithelial-mesenchymal transition. PLoS One **6:**e20804. doi:10.1371/journal.pone.0020804.
14. **Black AR, Black JD, Azizkhan-Clifford J.** 2001. Sp1 and Kruppel-like factor family of transcription factors in cell growth regulation and cancer. J. Cell. Physiol. **188:**143–160.
15. **Liu YN, Abou-Kheir W, Yin JJ, Fang L, Hynes P, Casey O, Hu D, Wan Y, Seng V, Sheppard-Tillman H, Martin P, Kelly K.** 2012. Critical and reciprocal regulation of KLF4 and SLUG in transforming growth factor beta-initiated prostate cancer epithelial-mesenchymal transition. Mol. Cell. Biol. **32:**941–953.
16. **Tiwari N, Meyer-Schaller N, Arnold P, Antoniadis H, Pachkov M, van Nimwegen E, Christofori G.** 2013. Klf4 is a transcriptional regulator of genes critical for EMT, including Jnk1 (Mapk8). PLoS One **8:**e57329. doi:10.1371/journal.pone.0057329.
17. **Zhang H, Liu L, Wang Y, Zhao G, Xie R, Liu C, Xiao X, Wu K, Nie Y, Zhang H, Fan D.** 2013. KLF8 involves in TGF-beta-induced EMT and promotes invasion and migration in gastric cancer cells. J. Cancer Res. Clin. Oncol. **139:**1033–1042.
18. **Wang X, Lu H, Urvalek AM, Li T, Yu L, Lamar J, DiPersio CM, Feustel PJ, Zhao J.** 2011. KLF8 promotes human breast cancer cell invasion and metastasis by transcriptional activation of MMP9. Oncogene **30:**1901–1911.
19. **Gumireddy K, Li A, Gimotty PA, Klein-Szanto AJ, Showe LC, Katsaros D, Coukos G, Zhang L, Huang Q.** 2009. KLF17 is a negative regulator of epithelial-mesenchymal transition and metastasis in breast cancer. Nat. Cell Biol. **11:**1297–1304.
20. **Ghaleb AM, Nandan MO, Chanchevalap S, Dalton WB, Hisamuddin IM, Yang VW.** 2005. Kruppel-like factors 4 and 5: the yin and yang regulators of cellular proliferation. Cell Res. **15:**92–96.
21. **Nakagawa M, Koyanagi M, Tanabe K, Takahashi K, Ichisaka T, Aoi T, Okita K, Mochiduki Y, Takizawa N, Yamanaka S.** 2008. Generation of induced pluripotent stem cells without Myc from mouse and human fibroblasts. Nat. Biotechnol. **26:**101–106.
22. **Guo P, Dong XY, Zhang X, Zhao KW, Sun X, Li Q, Dong JT.** 2009. Pro-proliferative factor KLF5 becomes anti-proliferative in epithelial homeostasis upon signaling-mediated modification. J. Biol. Chem. **284:**6071–6078.
23. **Xing C, Fu X, Sun X, Guo P, Li M, Dong JT.** 2013. Different expression patterns and functions of acetylated and unacetylated Klf5 in the proliferation and differentiation of prostatic epithelial cells. PLoS One **8:**e65538. doi:10.1371/journal.pone.0065538.
24. **Zeisberg M, Neilson EG.** 2009. Biomarkers for epithelial-mesenchymal transitions. J. Clin. Invest. **119:**1429–1437.
25. **Kalluri R, Weinberg RA.** 2009. The basics of epithelial-mesenchymal transition. J. Clin. Invest. **119:**1420–1428.
26. **Moreno-Bueno G, Peinado H, Molina P, Olmeda D, Cubillo E, Santos V, Palacios J, Portillo F, Cano A.** 2009. The morphological and molec-

ular features of the epithelial-to-mesenchymal transition. Nat. Protoc. **4:**1591–1613.
27. **Xu J, Lamouille S, Derynck R.** 2009. TGF-beta-induced epithelial to mesenchymal transition. Cell Res. **19:**156–172.
28. **Fuxe J, Vincent T, Garcia de Herreros A.** 2010. Transcriptional crosstalk between TGF-beta and stem cell pathways in tumor cell invasion: role of EMT promoting Smad complexes. Cell Cycle **9:**2363–2374.
29. **Brown KA, Aakre ME, Gorska AE, Price JO, Eltom SE, Pietenpol JA, Moses HL.** 2004. Induction by transforming growth factor-beta1 of epithelial to mesenchymal transition is a rare event in vitro. Breast Cancer Res. **6:**R215–R231.
30. **Davies M, Robinson M, Smith E, Huntley S, Prime S, Paterson I.** 2005. Induction of an epithelial to mesenchymal transition in human immortal and malignant keratinocytes by TGF-beta1 involves MAPK, Smad and AP-1 signalling pathways. J. Cell. Biochem. **95:**918–931.
31. **Nicoloso MS, Spizzo R, Shimizu M, Rossi S, Calin GA.** 2009. MicroRNAs—the micro steering wheel of tumour metastases. Nat. Rev. Cancer **9:**293–302.
32. **Gregory PA, Bert AG, Paterson EL, Barry SC, Tsykin A, Farshid G, Vadas MA, Khew-Goodall Y, Goodall GJ.** 2008. The miR-200 family and miR-205 regulate epithelial to mesenchymal transition by targeting ZEB1 and SIP1. Nat. Cell Biol. **10:**593–601.
33. **Korpal M, Lee ES, Hu G, Kang Y.** 2008. The miR-200 family inhibits epithelial-mesenchymal transition and cancer cell migration by direct targeting of E-cadherin transcriptional repressors ZEB1 and ZEB2. J. Biol. Chem. **283:**14910–14914.
34. **Park SM, Gaur AB, Lengyel E, Peter ME.** 2008. The miR-200 family determines the epithelial phenotype of cancer cells by targeting the E-cadherin repressors ZEB1 and ZEB2. Genes Dev. **22:**894–907.
35. **Kim T, Veronese A, Pichiorri F, Lee TJ, Jeon YJ, Volinia S, Pineau P, Marchio A, Palatini J, Suh SS, Alder H, Liu CG, Dejean A, Croce CM.** 2011. p53 regulates epithelial-mesenchymal transition through microRNAs targeting ZEB1 and ZEB2. J. Exp. Med. **208:**875–883.
36. **Kong W, Yang H, He L, Zhao JJ, Coppola D, Dalton WS, Cheng JQ.** 2008. MicroRNA-155 is regulated by the transforming growth factor beta/Smad pathway and contributes to epithelial cell plasticity by targeting RhoA. Mol. Cell. Biol. **28:**6773–6784.
37. **Zhang Z, Zhang B, Li W, Fu L, Fu L, Zhu Z, Dong JT.** 2011. Epigenetic silencing of miR-203 upregulates SNAI2 and contributes to the invasiveness of malignant breast cancer cells. Genes Cancer **2:**782–791.
38. **Bracken CP, Gregory PA, Kolesnikoff N, Bert AG, Wang J, Shannon MF, Goodall GJ.** 2008. A double-negative feedback loop between ZEB1-SIP1 and the microRNA-200 family regulates epithelial-mesenchymal transition. Cancer Res. **68:**7846–7854.
39. **Boukamp P, Petrussevska RT, Breitkreutz D, Hornung J, Markham A, Fusenig NE.** 1988. Normal keratinization in a spontaneously immortalized aneuploid human keratinocyte cell line. J. Cell Biol. **106:**761–771.
40. **Debnath J, Muthuswamy SK, Brugge JS.** 2003. Morphogenesis and oncogenesis of MCF-10A mammary epithelial acini grown in three-dimensional basement membrane cultures. Methods **30:**256–268.
41. **Aizawa K, Suzuki T, Kada N, Ishihara A, Kawai-Kowase K, Matsumura T, Sasaki K, Munemasa Y, Manabe I, Kurabayashi M, Collins T, Nagai R.** 2004. Regulation of platelet-derived growth factor-A chain by Kruppel-like factor 5: new pathway of cooperative activation with nuclear factor-kappaB. J. Biol. Chem. **279:**70–76.
42. **Chen C, Sun X, Ran Q, Wilkinson KD, Murphy TJ, Simons JW, Dong JT.** 2005. Ubiquitin-proteasome degradation of KLF5 transcription factor in cancer and untransformed epithelial cells. Oncogene **24:**3319–3327.
43. **Chen C, Bhalala HV, Qiao H, Dong JT.** 2002. A possible tumor suppressor role of the KLF5 transcription factor in human breast cancer. Oncogene **21:**6567–6572.
44. **Guo P, Dong XY, Zhao KW, Sun X, Li Q, Dong JT.** 2009. Opposing effects of KLF5 on the transcription of MYC in epithelial proliferation in the context of transforming growth factor beta. J. Biol. Chem. **284:**28243–28252.
45. **Guo P, Zhao KW, Dong XY, Sun X, Dong JT.** 2009. Acetylation of KLF5 alters the assembly of p15 transcription factors in transforming growth factor-beta-mediated induction in epithelial cells. J. Biol. Chem. **284:**18184–18193.
46. **Kao YC, Wu LW, Shi CS, Chu CH, Huang CW, Kuo CP, Sheu HM, Shi GY, Wu HL.** 2010. Downregulation of thrombomodulin, a novel target of Snail, induces tumorigenesis through epithelial-mesenchymal transition. Mol. Cell. Biol. **30:**4767–4785.
47. **Lichti U, Anders J, Yuspa SH.** 2008. Isolation and short-term culture of primary keratinocytes, hair follicle populations and dermal cells from newborn mice and keratinocytes from adult mice for in vitro analysis and for grafting to immunodeficient mice. Nat. Protoc. **3:**799–810.
48. **Chang CJ, Chao CH, Xia W, Yang JY, Xiong Y, Li CW, Yu WH, Rehman SK, Hsu JL, Lee HH, Liu M, Chen CT, Yu D, Hung MC.** 2011. p53 regulates epithelial-mesenchymal transition and stem cell properties through modulating miRNAs. Nat. Cell Biol. **13:**317–323.
49. **Xie D, Gore C, Liu J, Pong RC, Mason R, Hao G, Long M, Kabbani W, Yu L, Zhang H, Chen H, Sun X, Boothman DA, Min W, Hsieh JT.** 2010. Role of DAB2IP in modulating epithelial-to-mesenchymal transition and prostate cancer metastasis. Proc. Natl. Acad. Sci. U. S. A. **107:**2485–2490.
50. **Chen C, Benjamin MS, Sun X, Otto KB, Guo P, Dong XY, Bao Y, Zhou Z, Cheng X, Simons JW, Dong JT.** 2006. KLF5 promotes cell proliferation and tumorigenesis through gene regulation in the TSU-Pr1 human bladder cancer cell line. Int. J. Cancer **118:**1346–1355.
51. **Parisi S, Cozzuto L, Tarantino C, Passaro F, Ciriello S, Aloia L, Antonini D, De Simone V, Pastore L, Russo T.** 2010. Direct targets of Klf5 transcription factor contribute to the maintenance of mouse embryonic stem cell undifferentiated state. BMC Biol. **8:**128. doi:10.1186/1741-7007-8-128.
52. **Shinoda Y, Ogata N, Higashikawa A, Manabe I, Shindo T, Yamada T, Kugimiya F, Ikeda T, Kawamura N, Kawasaki Y, Tsushima K, Takeda N, Nagai R, Hoshi K, Nakamura K, Chung UI, Kawaguchi H.** 2008. Kruppel-like factor 5 causes cartilage degradation through transactivation of matrix metalloproteinase 9. J. Biol. Chem. **283:**24682–24689.
53. **Gregory PA, Bracken CP, Bert AG, Goodall GJ.** 2008. MicroRNAs as regulators of epithelial-mesenchymal transition. Cell Cycle **7:**3112–3118.
54. **Spaderna S, Brabletz T, Opitz OG.** 2009. The miR-200 family: central player for gain and loss of the epithelial phenotype. Gastroenterology **136:**1835–1837.
55. **Gill JG, Langer EM, Lindsley RC, Cai M, Murphy TL, Kyba M, Murphy KM.** 2011. Snail and the microRNA-200 family act in opposition to regulate epithelial-to-mesenchymal transition and germ layer fate restriction in differentiating ESCs. Stem Cells **29:**764–776.
56. **Chen J, Wang L, Matyunina LV, Hill CG, McDonald JF.** 2011. Overexpression of miR-429 induces mesenchymal-to-epithelial transition (MET) in metastatic ovarian cancer cells. Gynecol. Oncol. **121:**200–205.
57. **Miyoshi N, Ishii H, Nagano H, Haraguchi N, Dewi DL, Kano Y, Nishikawa S, Tanemura M, Mimori K, Tanaka F, Saito T, Nishimura J, Takemasa I, Mizushima T, Ikeda M, Yamamoto H, Sekimoto M, Doki Y, Mori M.** 2011. Reprogramming of mouse and human cells to pluripotency using mature microRNAs. Cell Stem Cell **8:**633–638.
58. **Wang G, Guo X, Hong W, Liu Q, Wei T, Lu C, Gao L, Ye D, Zhou Y, Chen J, Wang J, Wu M, Liu H, Kang J.** 2013. Critical regulation of miR-200/ZEB2 pathway in Oct4/Sox2-induced mesenchymal-to-epithelial transition and induced pluripotent stem cell generation. Proc. Natl. Acad. Sci. U. S. A. **110:**2858–2863.
59. **Burk U, Schubert J, Wellner U, Schmalhofer O, Vincan E, Spaderna S, Brabletz T.** 2008. A reciprocal repression between ZEB1 and members of the miR-200 family promotes EMT and invasion in cancer cells. EMBO Rep. **9:**582–589.
60. **Thiery JP.** 2003. Epithelial-mesenchymal transitions in development and pathologies. Curr. Opin. Cell Biol. **15:**740–746.
61. **Nieto MA.** 2011. The ins and outs of the epithelial to mesenchymal transition in health and disease. Annu. Rev. Cell Dev. Biol. **27:**347–376.
62. **Taylor MA, Parvani JG, Schiemann WP.** 2010. The pathophysiology of epithelial-mesenchymal transition induced by transforming growth factor-beta in normal and malignant mammary epithelial cells. J. Mammary Gland Biol. Neoplasia **15:**169–190.
63. **Moustakas A, Heldin CH.** 2007. Signaling networks guiding epithelial-mesenchymal transitions during embryogenesis and cancer progression. Cancer Sci. **98:**1512–1520.
64. **Cao L, Feng C, Li L, Zuo Z.** 2012. Contribution of microRNA-203 to the isoflurane preconditioning-induced neuroprotection. Brain Res. Bull. **88:**525–528.
65. **Jin J, Deng J, Wang F, Xia X, Qiu T, Lu W, Li X, Zhang H, Gu X, Liu Y, Cao W, Shao W.** 2013. The expression and function of microRNA-203 in lung cancer. Tumour Biol. **34:**349–357.
66. **Chen Y, Xiao Y, Ge W, Zhou K, Wen J, Yan W, Wang Y, Wang B, Qu C, Wu J, Xu L, Cai W.** 2013. miR-200b inhibits TGF-beta1-induced epithelial-mesenchymal transition and promotes growth of intestinal epithelial cells. Cell Death Dis. **4:**e541. doi:10.1038/cddis.2013.22.

67. **Hurteau GJ, Carlson JA, Roos E, Brock GJ.** 2009. Stable expression of miR-200c alone is sufficient to regulate TCF8 (ZEB1) and restore E-cadherin expression. Cell Cycle **8:**2064–2069.
68. **Craig VJ, Cogliatti SB, Rehrauer H, Wundisch T, Muller A.** 2011. Epigenetic silencing of microRNA-203 dysregulates ABL1 expression and drives Helicobacter-associated gastric lymphomagenesis. Cancer Res. **71:** 3616–3624.
69. **Yang Y, Ahn YH, Gibbons DL, Zang Y, Lin W, Thilaganathan N, Alvarez CA, Moreira DC, Creighton CJ, Gregory PA, Goodall GJ, Kurie JM.** 2011. The Notch ligand Jagged2 promotes lung adenocarcinoma metastasis through a miR-200-dependent pathway in mice. J. Clin. Invest. **121:**1373–1385.
70. **Arima Y, Hayashi H, Sasaki M, Hosonaga M, Goto TM, Chiyoda T, Kuninaka S, Shibata T, Ohata H, Nakagama H, Taya Y, Saya H.** 2012. Induction of ZEB proteins by inactivation of RB protein is key determinant of mesenchymal phenotype of breast cancer. J. Biol. Chem. **287:** 7896–7906.
71. **Primo MN, Bak RO, Schibler B, Mikkelsen JG.** 2012. Regulation of pro-inflammatory cytokines TNFalpha and IL24 by microRNA-203 in primary keratinocytes. Cytokine **60:**741–748.
72. **Ahn SM, Cha JY, Kim J, Kim D, Trang HT, Kim YM, Cho YH, Park D, Hong S.** 2012. Smad3 regulates E-cadherin via miRNA-200 pathway. Oncogene **31:**3051–3059.
73. **Verschueren K, Remacle JE, Collart C, Kraft H, Baker BS, Tylzanowski P, Nelles L, Wuytens G, Su MT, Bodmer R, Smith JC, Huylebroeck D.** 1999. SIP1, a novel zinc finger/homeodomain repressor, interacts with Smad proteins and binds to 5′-CACCT sequences in candidate target genes. J. Biol. Chem. **274:**20489–20498.
74. **Mizuguchi Y, Specht S, Lunz JG, III, Isse K, Corbitt N, Takizawa T, Demetris AJ.** 2012. Cooperation of p300 and PCAF in the control of microRNA 200c/141 transcription and epithelial characteristics. PLoS One **7:**e32449. doi:10.1371/journal.pone.0032449.
75. **Wellner U, Schubert J, Burk UC, Schmalhofer O, Zhu F, Sonntag A, Waldvogel B, Vannier C, Darling D, Azur Hausen Brunton VG, Morton J, Sansom O, Schuler J, Stemmler MP, Herzberger C, Hopt U, Keck T, Brabletz S, Brabletz T.** 2009. The EMT-activator ZEB1 promotes tumorigenicity by repressing stemness-inhibiting microRNAs. Nat. Cell Biol. **11:**1487–1495.
76. **Kong D, Banerjee S, Ahmad A, Li Y, Wang Z, Sethi S, Sarkar FH.** 2010. Epithelial to mesenchymal transition is mechanistically linked with stem cell signatures in prostate cancer cells. PLoS One **5:**e12445. doi:10.1371/journal.pone.0012445.
77. **McKenna DJ, McDade SS, Patel D, McCance DJ.** 2010. MicroRNA 203 expression in keratinocytes is dependent on regulation of p53 levels by E6. J. Virol. **84:**10644–10652.
78. **Xia H, Cheung WK, Sze J, Lu G, Jiang S, Yao H, Bian XW, Poon WS, Kung HF, Lin MC.** 2010. miR-200a regulates epithelial-mesenchymal to stem-like transition via ZEB2 and beta-catenin signaling. J. Biol. Chem. **285:**36995–37004.
79. **Lim Y, Wright JA, Attema JL, Gregory PA, Bert AG, Smith E, Thomas D, Drew PA, Khew-Goodall Y, Goodall GJ.** 2013. Epigenetic modulation of the miR-200 family is associated with transition to a breast cancer stem-cell-like state. J. Cell Sci. **126**(Pt 10)**:**2256–2266.
80. **Nakajima Y, Akaogi K, Suzuki T, Osakabe A, Yamaguchi C, Sunahara N, Ishida J, Kako K, Ogawa S, Fujimura T, Homma Y, Fukamizu A, Murayama A, Kimura K, Inoue S, Yanagisawa J.** 2011. Estrogen regulates tumor growth through a nonclassical pathway that includes the transcription factors ERbeta and KLF5. Sci. Signal. **4:**ra22. doi:10.1126/scisignal.2001551.
81. **Nagamatsu G, Kosaka T, Saito S, Honda H, Takubo K, Kinoshita T, Akiyama H, Sudo T, Horimoto K, Oya M, Suda T.** 2013. Induction of pluripotent stem cells from primordial germ cells by single reprogramming factors. Stem Cells **31:**479–487.
82. **Bourillot PY, Savatier P.** 2010. Kruppel-like transcription factors and control of pluripotency. BMC Biol. **8:**125. doi:10.1186/1741-7007-8-125.
83. **Ema M, Mori D, Niwa H, Hasegawa Y, Yamanaka Y, Hitoshi S, Mimura J, Kawabe Y, Hosoya T, Morita M, Shimosato D, Uchida K, Suzuki N, Yanagisawa J, Sogawa K, Rossant J, Yamamoto M, Takahashi S, Fujii-Kuriyama Y.** 2008. Kruppel-like factor 5 is essential for blastocyst development and the normal self-renewal of mouse ESCs. Cell Stem Cell **3:**555–567.
84. **Jiang J, Chan YS, Loh YH, Cai J, Tong GQ, Lim CA, Robson P, Zhong S, Ng HH.** 2008. A core Klf circuitry regulates self-renewal of embryonic stem cells. Nat. Cell Biol. **10:**353–360.
85. **Parisi S, Passaro F, Aloia L, Manabe I, Nagai R, Pastore L, Russo T.** 2008. Klf5 is involved in self-renewal of mouse embryonic stem cells. J. Cell Sci. **121:**2629–2634.
86. **Lin SC, Wani MA, Whitsett JA, Wells JM.** 2010. Klf5 regulates lineage formation in the pre-implantation mouse embryo. Development **137:** 3953–3963.
87. **Lehman TA, Modali R, Boukamp P, Stanek J, Bennett WP, Welsh JA, Metcalf RA, Stampfer MR, Fusenig N, Rogan EM, Harris CC.** 1993. p53 mutations in human immortalized epithelial cell lines. Carcinogenesis **14:**833–839.
88. **Merlo GR, Basolo F, Fiore L, Duboc L, Hynes NE.** 1995. p53-dependent and p53-independent activation of apoptosis in mammary epithelial cells reveals a survival function of EGF and insulin. J. Cell Biol. **128:**1185–1196.